Supplements to :

Population Ecology from Local to Global Scales: a case study using *Plantago lanceolata*

by

Maude E. A. Baudraz

MSc., Behaviour, Evolution and Conservation, University of Lausanne, 2015

A thesis submitted in partial fulfilment of

the requirements for the degree of

Doctor of Philosophy

School of Natural Sciences (Zoology)

Trinity College Dublin

The University of Dublin

2022

Table of contents

List of Figures

List of Tables

Supplements to: Chapter 1 What is size ? - size variable selection for demographic studies at global scales

Supplement S1.1, Supplement to Methods

S.1.1.1 Details of the dataset version used for this study.

The data curation of the PlantPopNet network includes the thorough cleaning of incoming data for mistakes made upon measurement in the field or during data entry. Once cleaned, year after year, new field data is added to the existing database. For reproducibility purposes, it is therefore necessary to include information referring to the exact version of the dataset used, as any subsequent data curation, subsetting or changes performed.

In this project, we used the PLANTPOPNET_Y0_V1.02_2020-11-18 and PLANTPOPNET_Y1_V1.1_2021-03-31 datasheets (standard data products). In addition, we performed the following data cleaning steps: population CDF was excluded, as the number of individuals indicated as surviving in year 1 did not match the numbers of individuals alive in year 0 and year 2. We excluded individuals LK1_T1_P8_121, LK1_T1_P8_122 as there was apparently a shift in the columns of the leaf measurements; these plants had the highest observed number of leaves in the whole dataset, but no leaf width information. We excluded observations of 305, 300 and 240 floral stems per rosette, as they were paired with leaf width <3mm and were probably due to column shifts again. These extremely high number of floral stems values stemmed from the same year and population as the extreme number of leaves values. Other high number of stems or leaf values were maintained, as there was no evidence of any mistake. These corrections take place in a dataset including 18146 observations of rosettes.

S.1.1.2 Details of the biomass equation

The biomass equation was developed following the method of Villellas et al. (2021). They harvested aerial biomass information from 396 specimen grown in the greenhouse seeds stemming from 16 populations included in the present study. They established a regression equation to predict aerial biomass from the leaf measurements collected in the field (leaf number, length and width), which we are reusing here. They applied Linear Mixed Models and model selection based on Akaike Information Criterion for finite sample sizes (AIC_c). Aboveground dry biomass was the response variable, and they compared AIC_c values of models with all possible combinations of main effects of leaf length, leaf width, leaf number and the square term of the number of leaves as explanatory variables (no interactions). In all models, all variables except leaf length were log-transformed to normalise distribution of errors, and population of origin, as well as the light condition the plants

were grown under in Villellas et al., were included as a random effect. The model including all three variables and the square term of the number of leaves provided the lowest AIC_c and an is strongly supported by the data (conditional R2 0.86). The resulting equation is as follows:

$$e^{0.5559346+1.9239234*\log(n°leaves)-0.2128901*\log(n°leaves)^2+0.0028415*leaf\ length+\ 0.8332087*\log\ (leaf\ width)}$$

Analyses were performed with the packages *lme4* (Bates *et al*. 2015) and *MuMIn* (Barton 2016) in R software (R Core Team 2017). We refer the reader to (Villellas et al. 2021) for more details about the greenhouse conditions and light treatments.

S.1.1.3 Evaluation of the models – choice of performance metrics

We made use of two different performance metrics; an R^2 adapted to generalized linear mixed models (Johnson 2014; Nakagawa, Johnson, and Schielzeth 2017; Nakagawa and Schielzeth 2013), and the Mean Absolute Error (MAE; Chai and Draxler, 2014; Cort J. Willmott and Matsuura, 2005). Nakagawa's R^2 is divided into conditional and marginal R^2. Marginal R^2 (R^2_m) can be understood as the variance explained by the fixed effects in the model, while the conditional R^2 (R^2_c) is the variance explained by the entire model including the random structure. We used R^2 as an overall metric of model performance, and MAE as a way to investigate further the error of the model in each separate population.

The Mean Absolute Error is computed as follow:

$$MAE = \frac{\sum_i^n |e_i|}{n} \qquad \textbf{eqn 3}$$

Where e_i is the *i*-th model error of a model with *n* observations.

To obtain MAE values comparable between models calibrated on different responses, we mean centred and standardized the residuals of all models and calculated the MAE based on those standardized residuals.

Both these metrics were selected on the following basis; they provide information about the performance of the model (Chai and Draxler 2014; Nakagawa and Schielzeth 2013), they are applicable to mixed models and to the different error families we make use of in this study (Chai and Draxler 2014; Nakagawa et al. 2017), they can be compared between models with different response variables, even if these have been built on different datasets (unlike selection criteria such as AIC; Nakagawa and Schielzeth (2013) and between error distributions (although this is a bit more arduous; Nakagawa et al. (2017). We preferred MAE to the Root Mean Squared Error (RMSE), as MAE is more intuitive, as it is linked directly to the absolute error of the models. Furthermore, although there is evidence that RMSE should be favoured in the cases where the error is expected

to be normal (Chai and Draxler 2014), we want to compare various types of models with different error families, in which case MAE is advised (Willmott and Matsuura 2005). Finally, both R^2 and MAE are easily interpretable.

S.1.1.4 Evaluation of the models – the Dharma protocol

The DARHMa methodology (Hartig 2020) simulates a set of expected residuals based on the model and assuming the assumptions are met. The dharma residuals are then the difference between the simulated and the actual residuals. These "DHARMa residuals" then have to meet the assumptions of uniformity, and overdispertion of the residuals can be tested. The vignette of the package is extremely well furnished and we invite all to read it for more details; https://cran.r-project.org/web/packages/DHARMa/vignettes/DHARMa.html. The functions used here were slightly adapted, so that they do not display p-values (as we diagnose multiple models).

Supplement S1.2: Illustration of the approach used to explore the model diagnostics of the vital rate models under criterion a)

The following graphs illustrate the model diagnostic approach followed for criterion a. We made use of the Dharma methodology for the exploration of generalized linear mixed models developed and its related R package (Hartig 2020).

We present the plots stemming from two of our models as examples: one good one (the survival model using the untransformed number of leaves as a size predictor) and one which we described as "suboptimal" in the main text (the growth model making use of the log transformed length of the longest leaf as a size metric). For details about the interpretation of these plots, see section S1.1.4.

Supplement S1.2.1 Example of a model with good Dharma diagnostics

The following shows the details of the summary of the model, followed by the plots from the Dharma diagnostics approach.

no_leaves_Y0

Formula of the model:
survived_Y1 ~ no_leaves_Y0 + (no_leaves_Y0 | site_code) + (1 | unique_plot_ID) <environment: 0x7fec19def2c8>

Summary table:

Diagnotsics:
MODEL INFO: Observations: 5746 Dependent Variable: survived_Y1 Type: Mixed effects generalized linear regression Error Distribution: binomial Link function: logit

MODEL FIT: AIC = 5072.32, BIC = 5112.26 Pseudo-R^2 (fixed effects) = 0.21 Pseudo-R^2 (total) = 0.72

FIXED EFFECTS:

	Est.	S.E.	z val.	p
(Intercept)	0.66	0.22	2.96	0.00
no_leaves_Y0	0.19	0.04	5.50	0.00

RANDOM EFFECTS:

Group	Parameter	Std. Dev.
unique_plot_ID	(Intercept)	0.81
site_code	(Intercept)	1.33
site_code	no_leaves_Y0	0.17

Grouping variables:

Group	# groups	ICC
unique_plot_ID	658	0.11
site_code	54	0.31

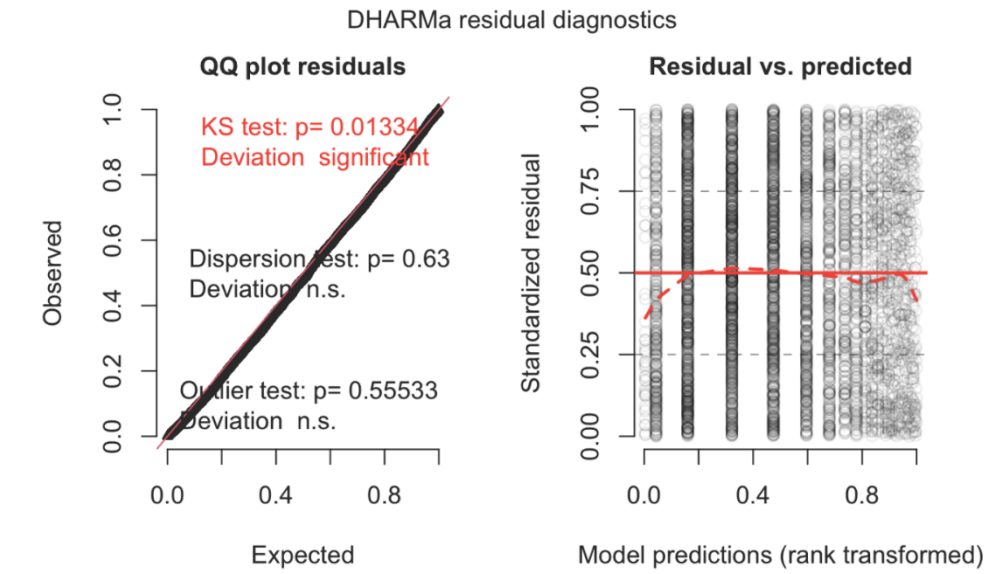
DHARMa residual diagnostics
QQ plot residuals
KS test: p= 0.01334
Deviation significant
Dispersion test: p= 0.63
Deviation n.s.
Outlier test: p= 0.55533
Deviation n.s.
Observed
Expected
Residual vs. predicted
Standardized residual
Model predictions (rank transformed)

NULL

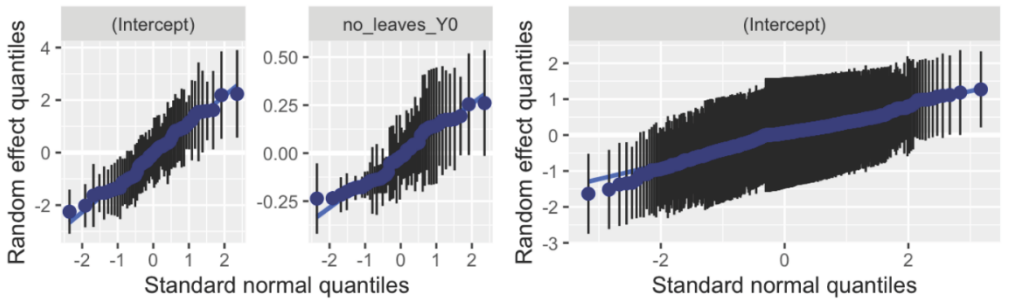
(Intercept)
no_leaves_Y0
Random effect quantiles
Standard normal quantiles
(Intercept)
Random effect quantiles
Standard normal quantiles

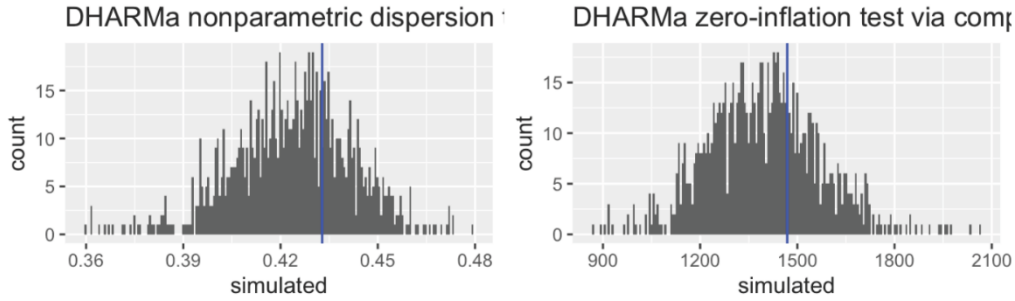
DHARMa nonparametric dispersion
count
simulated
DHARMa zero-inflation test via comp
count
simulated

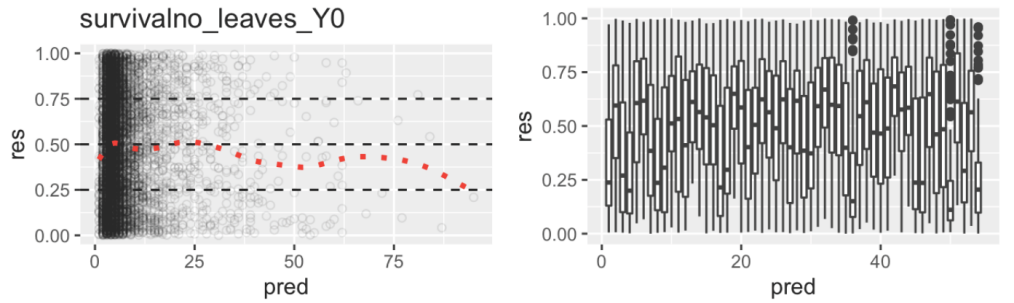
survivalno_leaves_Y0
res
pred
res
pred

Supplement S1.2.2 Example of a model with poorer Dharma diagnostics

Log_longest_leaf_Y0

Formula of the model:
Log_longest_leaf_Y1 ~ Log_longest_leaf_Y0 + (Log_longest_leaf_Y0 | site_code) + (1 | unique_plot_ID)
<environment: 0x7fed0055e5a0>

Summary table:

Diagnotsics:
MODEL INFO: Observations: 4321 Dependent Variable: Log_longest_leaf_Y1 Type: Mixed effects linear regression

MODEL FIT: AIC = 3386.28, BIC = 3430.88 Pseudo-R^2 (fixed effects) = 0.24 Pseudo-R^2 (total) = 0.68

FIXED EFFECTS:

	Est.	S.E.	t val.	d.f.	p
(Intercept)	2.54	0.20	12.67	52.59	0.00
Log_longest_leaf_Y0	0.49	0.04	12.66	52.87	0.00

p values calculated using Kenward-Roger standard errors and d.f.

RANDOM EFFECTS:

Group	Parameter	Std. Dev.
unique_plot_ID	(Intercept)	0.16
site_code	(Intercept)	1.31

Group	Parameter	Std. Dev.
site_code	Log_longest_leaf_Y0	0.25
Residual		0.33

Grouping variables:

Group	# groups	ICC
unique_plot_ID	602	0.01
site_code	55	0.93

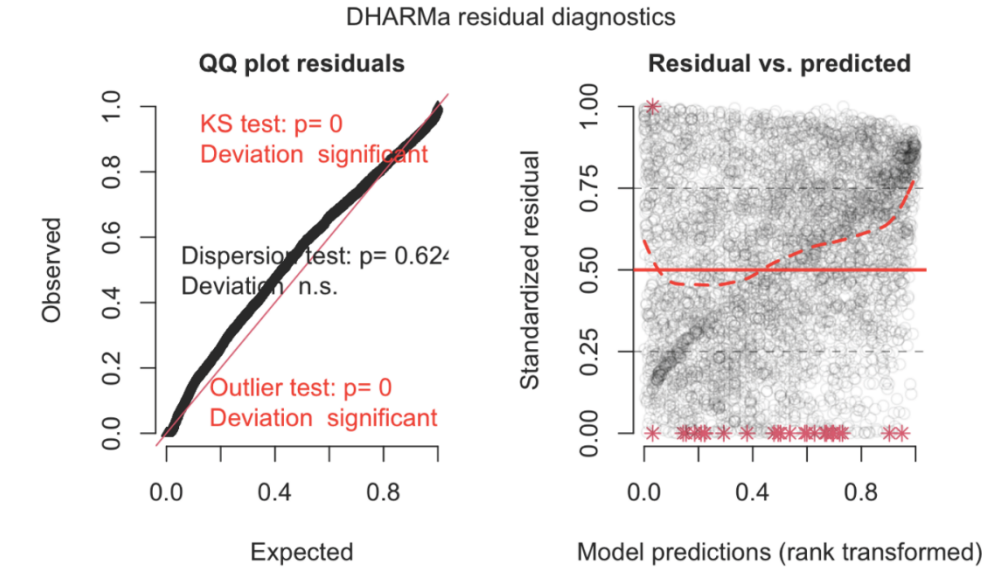
DHARMa residual diagnostics
QQ plot residuals
KS test: p= 0
Deviation significant
Dispersion test: p= 0.624
Deviation n.s.
Outlier test: p= 0
Deviation significant
Observed
Expected
Residual vs. predicted
Standardized residual
Model predictions (rank transformed)

NULL

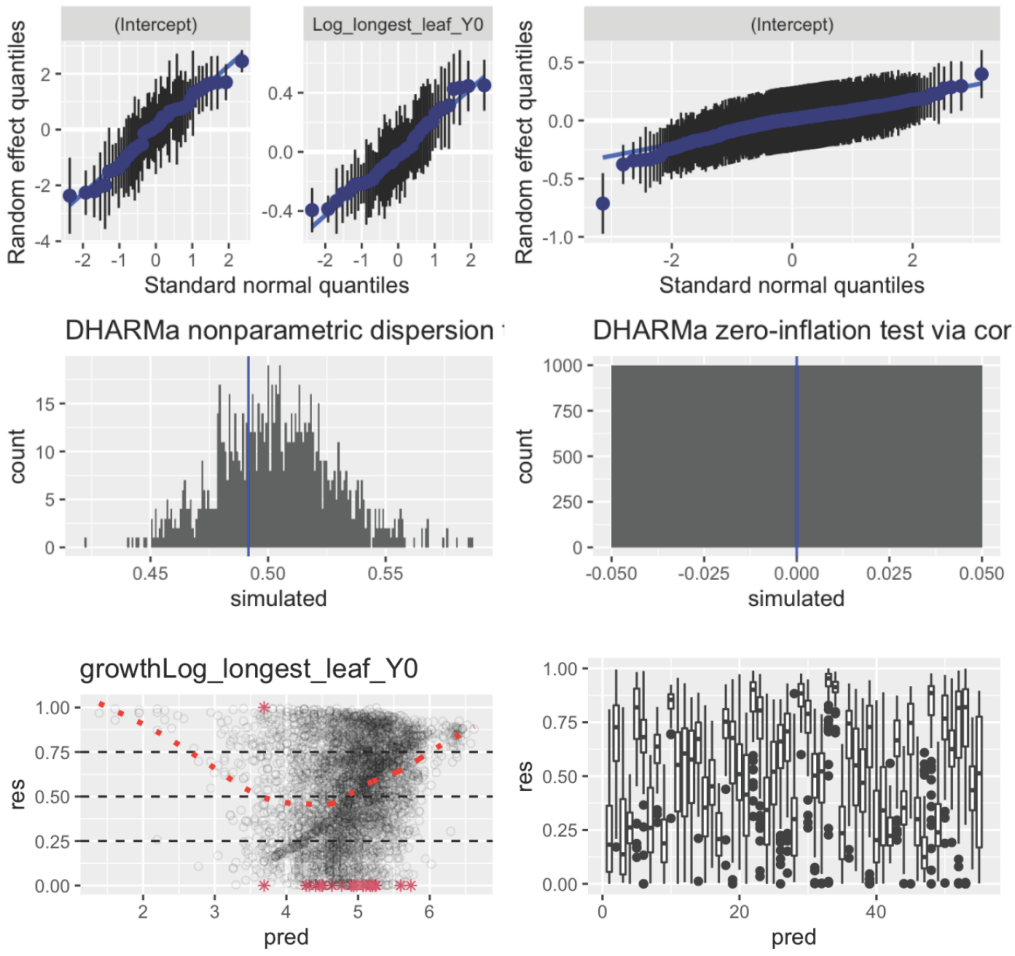
(Intercept)
Log_longest_leaf_Y0
Random effect quantiles
Standard normal quantiles
(Intercept)
Random effect quantiles
Standard normal quantiles
DHARMa nonparametric dispersion
count
simulated
DHARMa zero-inflation test via cor
count
simulated
growthLog_longest_leaf_Y0
res
pred
res
pred

A

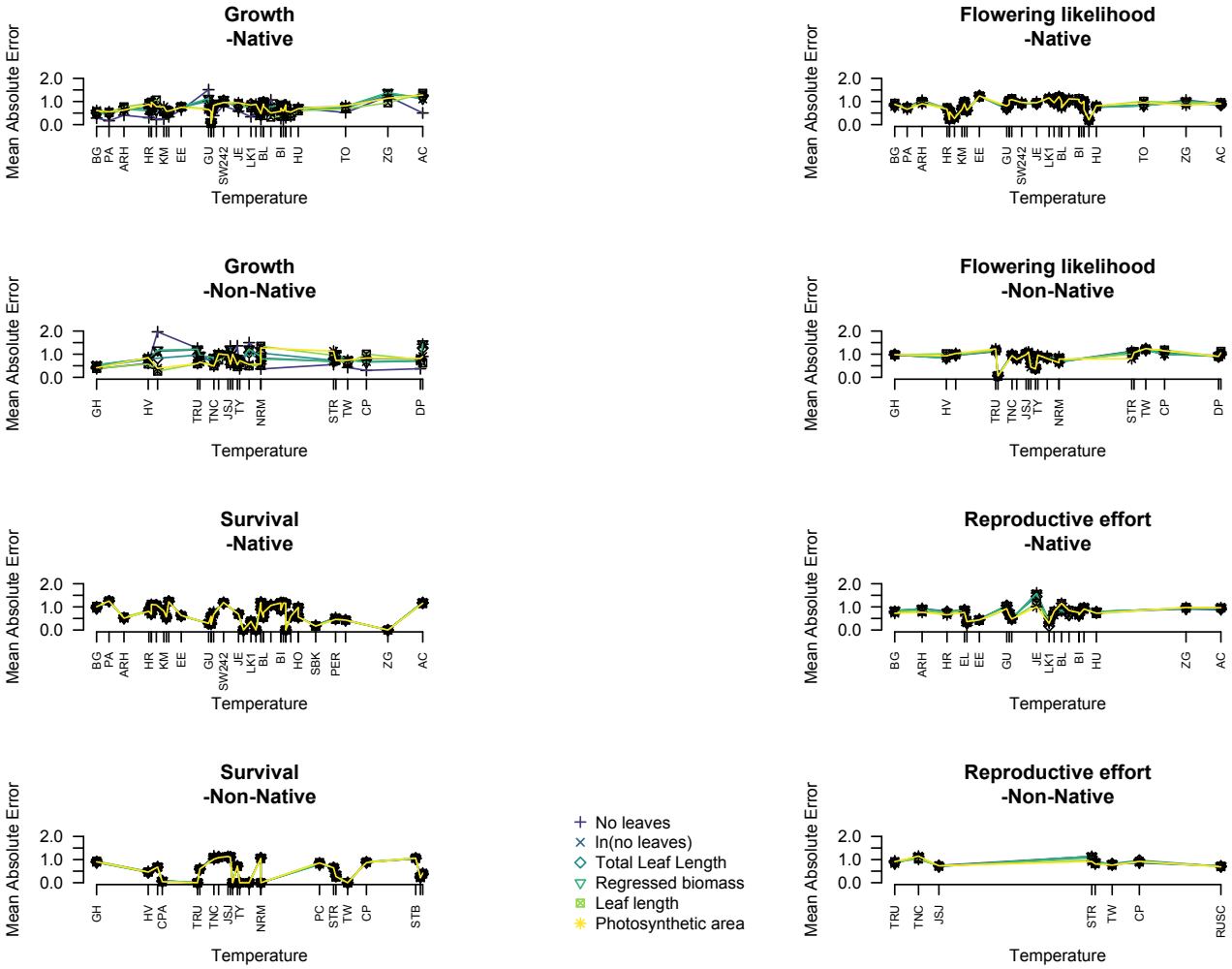

Figure S1.3.1 Patterns of Mean Average Error along two main climatic gradients; A) temperature and B) precipitation (displayed on the next page). *Upper rows show the native range populations, lower rows the non-native range. Populations are on the x-axis, placed by order of increasing A) temperature and B) precipitation. Y-axis shows the Mean Absolute Error (ratio of the sum of the absolute value of the residuals over the number of observation) in this population. Each symbol and color represents a different size metric (see legend). Highly differentiated lines would show a strong difference between the three candidate size metrics in their performance. High differences between Mean Absolute Error for different populations show a strong difference in performance at the population level. In the present case, size metrics mostly perform so similarly that the lines confound and overlap.*

B

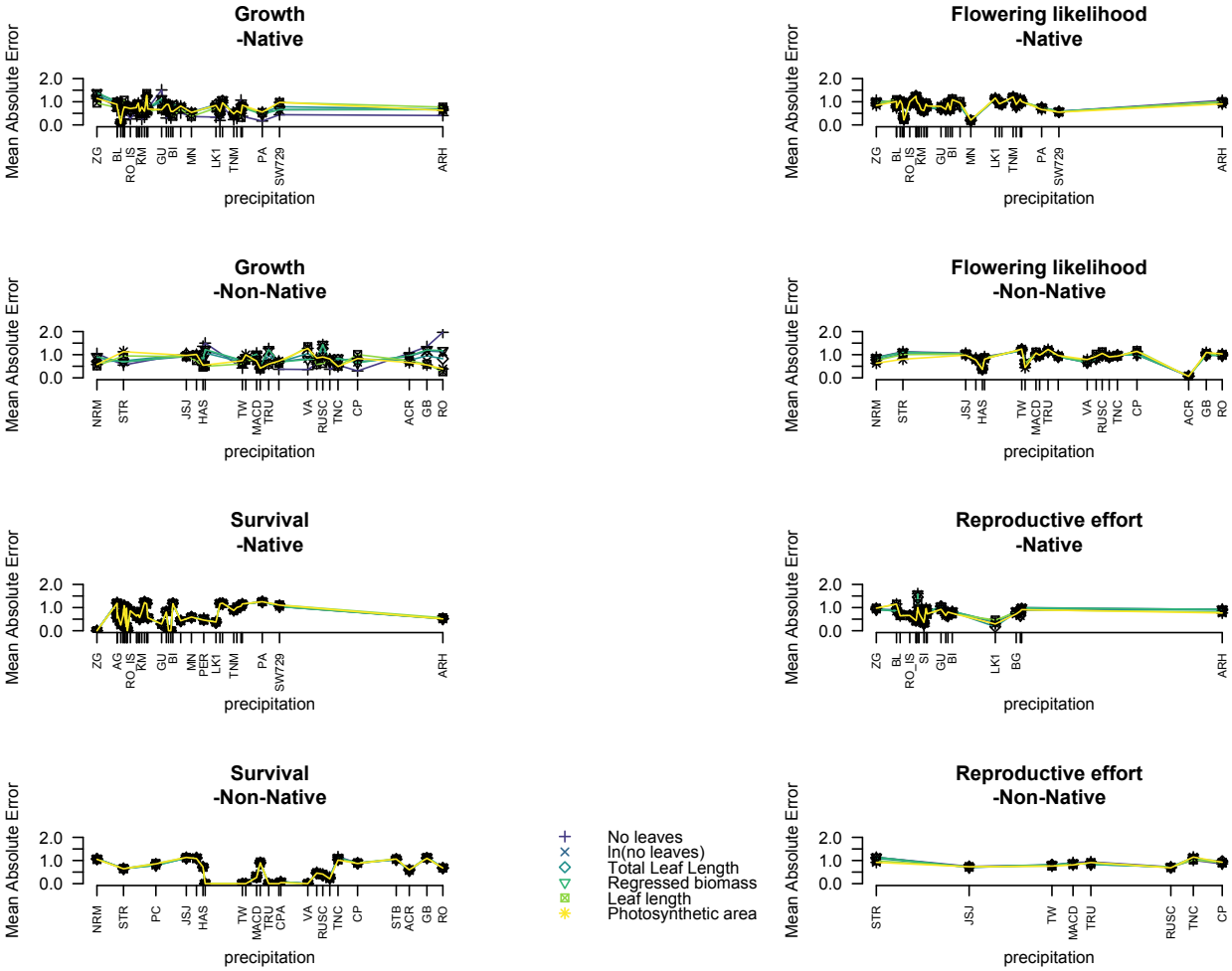
Growth
-Native
Mean Absolute Error
2.0
1.0
0.0
ZG BL RO_IS RM GU BI MN LK1 TNM PA SW729 ARH
precipitation
Flowering likelihood
-Native
Mean Absolute Error
2.0
1.0
0.0
ZG BL RO_IS RM GU BI MN LK1 TNM PA SW729 ARH
precipitation
Growth
-Non-Native
Mean Absolute Error
2.0
1.0
0.0
NRM STR JSJ HAS TW MACD TRU VA RUSC TNC CP ACR GB RO
precipitation
Flowering likelihood
-Non-Native
Mean Absolute Error
2.0
1.0
0.0
NRM STR JSJ HAS TW MACD TRU VA RUSC TNC CP ACR GB RO
precipitation
Survival
-Native
Mean Absolute Error
2.0
1.0
0.0
ZG AG RO_IS RM GU BI MN PER LK1 TNM PA SW729 ARH
precipitation
Reproductive effort
-Native
Mean Absolute Error
2.0
1.0
0.0
ZG BL RO_IS SI GU BI LK1 BG ARH
precipitation
Survival
-Non-Native
Mean Absolute Error
2.0
1.0
0.0
NRM STR PC JSJ HAS TW MACD TRU CPA VA RUSC TNC CP STB ACR GB RO
precipitation
No leaves
ln(no leaves)
Total Leaf Length
Regressed biomass
Leaf length
Photosynthetic area
Reproductive effort
-Non-Native
Mean Absolute Error
2.0
1.0
0.0
STR JSJ TW MACD TRU RUSC TNC CP
precipitation

Supplement S1.3.2: Effect of size metric, temperature and precipitation on MAE

MODEL INFO:
Observations: 196
Dependent Variable: MAE
Type: Mixed effects linear regression

MODEL FIT:
AIC = -227.17, BIC = -187.83
Pseudo-R^2 (fixed effects) = 0.05
Pseudo-R^2 (total) = 0.88

FIXED EFFECTS:

	Est.	S.E.	t val.	d.f.	p
(Intercept)	0.76	0.06	12.44	27.21	0.00
size metric (no leaves)	0.04	0.02	1.57	162.00	0.12
size metric (ln(no leaves))	0.04	0.02	1.82	162.00	0.07
size metric (Total Leaf Length)	0.03	0.02	1.30	162.00	0.19
size metric (regressed biomass)	0.04	0.02	1.83	162.00	0.07
size metric (longest leaf)	0.02	0.02	0.95	162.00	0.34
size metric (photosynthetic area)	0.00	0.02	0.18	162.00	0.85
precipitation	0.01	0.05	0.23	24.00	0.82
temperature	0.05	0.06	0.71	24.00	0.48
RangeNon-Native	0.02	0.14	0.17	24.00	0.87

p values calculated using Kenward-Roger standard errors and d.f.

RANDOM EFFECTS:

Group	Parameter	Std. Dev.
pop	(Intercept)	0.23
Residual		0.09

Grouping variables:

Group	# groups	ICC
pop	28	0.87

Supplements to: Chapter 2 Vital rate and life history strategies of P. lanceolata are captured by SDM predicted suitability along a steep environmental gradient in the Swiss Alps

Supplement S2.1 Supplement to the main text

Supplementary material S2.1.1: added information on the SDM

Water availability, temperature and neighbouring vegetation cover or height are described as the best descriptors of several ecological processes for *P. lanceolata* (Kuiper and Bos 1992). Kuiper and Bos (1992) also highlighted the high importance of land use, such as agricultural use or disturbance, and soil physical properties in driving the distribution of the species (see as well publication such as Kozáková et al., 2015). Soil chemical properties, on the other hand, were shown to be of little relevance to the distribution of *P. lanceolata* L. (Kuiper and Bos 1992; Wu and Antonovics 1976). As a result, two climatic predictors (yearly moisture index, yearly mean temperature), two topographic predictors (slope and topographic position) and one biotic predictor (vegetation height) were included in our model. The environmental predictors used are detailed in Table 1. All variables were cropped to exclude forested areas.

No layer of agricultural use information was available for the study area at the time of this study. Nonetheless, in this mountain area, both land use and soil properties are highly linked to the steepness of the slope and the position within the topography of the soil (Randin et al. 2009). Slope and flatness of the terrain will affect the exploitation type and choice, and bumpiness of the terrain will create places of more intensive exploitation or grazing. The same variables will affect nutrient deposition and soil depth on steep mountainsides (Körner 2003). Slope and topographic position were hence added as surrogates for soil properties and land use in the research area. The slope is measured in degrees and derived from the digital elevation model (DEM) with ArcGis 9.3 spatial analyst tool (Dubuis, Giovanettina, et al. 2013). The topographic position is computed with moving windows and is an integration of topographic features at various scales; positive values of this variable indicate ridges and tops and negative values valleys and sinks (Dubuis, Giovanettina, et al. 2013). This variable was calculated using the method of Zimmermann, Edwards, Moisen, Frescino, and Blackward (2007).

Water availability and temperature were captured via layers of yearly moisture index and yearly mean temperature (Dubuis, Rossier, et al. 2013; Zimmermann and Kienast 1999). These climatic predictors were computed from the monthly means of the average temperature (°C) and sum of precipitation (mm) data recorded between 1961 and 1990 by the Swiss network of meteorological stations (www.meteosuisse.ch), using only the information from the growing season (June-August). The point measurement are interpolated on Switzerland with local thin-plate spline-functions for temperature and a regionalized linear regression model for precipitation based on a digital elevation model (from the Swiss Federal Office of Topography, www.swisstopo.ch) (Zimmermann and Kienast 1999). The moisture index is the mean difference between precipitation and potential evapotranspiration over the growing season and represents the amount of water potentially available in the soil.

As the height of the neighbouring vegetation was shown to have a high impact on the distribution of *P. lanceolata* L., we used a modelled layer of coverage weighted mean community vegetation height developed for the study area (Baudraz et al. 2018). This layer was developed using exhaustive community inventories and species specific mean functional traits value sampled in the same study area (Dubuis, Rossier, et al. 2013). Using this data, Baudraz et al., (2018) interpolated the coverage weighted mean community vegetative height of non-forested areas over the whole research area. We used this layer as a way to capture vegetation height in the study area.

We used Biomod2 to fit the individual SDMs and derive the final prediction of habitat suitability (Thuiller et al. 2016). The three following modelling techniques were included in the ensemble: boosted regression trees (BRT; (Elith, Leathwick, and Hastie 2008), random forest (RF; Prasad, Iverson, & Liaw, 2006) and generalized linear model (GLM; Guisan, Edwards, & Hastie, 2002). The models and the final prediction were evaluated through repeated split sampling (models calibrated on 70% of the data, and evaluated on 30%) using AUC, max-Kappa and max-TSS (Guisan, Thuiller, and Zimmermann 2017). A final, ensemble model using all of the data was then projected over the study area and used as an environmental suitability metric in the rest this study (Guisan et al. 2017).

Supplementary material S2.1.2: added information on the site selection

The suitability range (from min to max log odds value) was divided into five strata each covering 20% of all possible suitability values. Seven known *P. lanceolata* occurrences in each stratum were

randomly selected as candidate sites. Candidate sites were visited over the first fieldwork season (June-August 2017). If the occurrence of *P. lanceolata* was confirmed and the site deemed suitable for the PlantPopNet protocol (Buckley et al. 2019), a population monitoring site was set up. In total, 19 populations were set up, four in each suitability stratum except for the lowest suitability. In the latter, some reported occurrences were actually misidentifications of the species *P. atrata*, and only three populations could be set up. In another stratum, a candidate site was discarded as it did not match the criteria for the establishment of a PlantPopNet population (foreseeable sudden change in land use in the next few years; Buckley et al. 2019), but could be replaced by another suitable candidate site. The data of one site at the middle range of values had to be discarded, as plants marked in the first year could not be consistently relocated in future years.

Supplementary material S2.1.2: Fieldwork and gathering of demographic data

Setting up of the populations, demographic census and collection of functional traits data were performed following the PlantPopNet protocol (Buckley et al. 2019). In Summer (June-August) 2017, 100 individuals per site were mapped and tagged using small linoleum squares, fixed in the ground at the foot of each plant with a plastic coated metallic pin. This enabled us to find them accurately in subsequent years. The size (number of leaves and length/width of the longest leaf) and reproductive effort (number of stems and inflorescence length) of each rosette of each individual were recorded during the summer for three years (2017-2019). When new individual rosettes were produced, they were also tagged and measured, and given an individual identifier, either within the genet they belonged to or as separate, new recruits. Seedlings were counted, but not marked until their second year, to avoid tagging related mortality. Repeated demographic censuses at each site enabled the calculation of rates of reproduction, growth of each rosette and individual, recruitment in the population and mortality/survival of adult individuals.

Supplement S2.2 Supplementary Figures

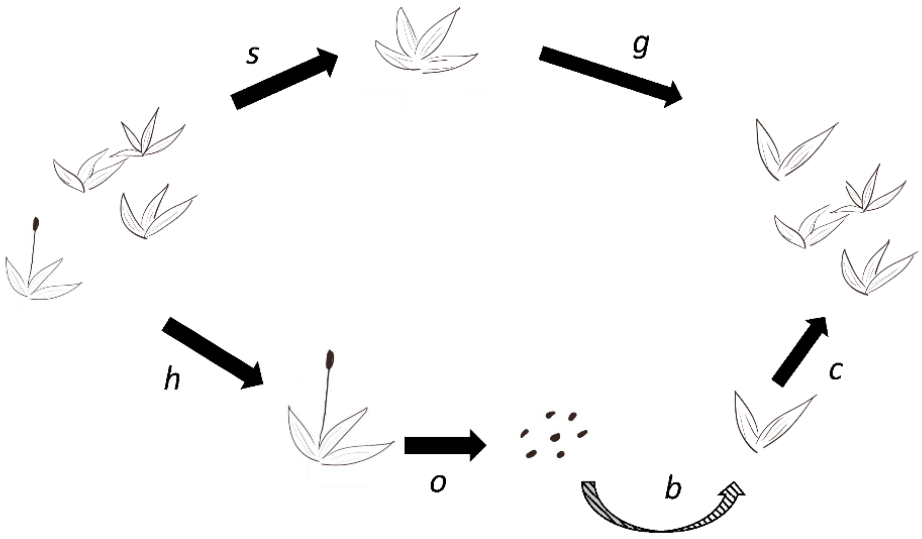

Figure S2.2.1: life cycle of the focal species. *An individual of size* z_t *at time t can contribute to the population at time t+1 by either surviving (*s*) and growing or shrinking (*g*) to a size* z_{t+1}*, or entering a reproductive event starting by flowering with a probability of* h*, then producing a certain reproductive effort (*o*, measured in mm of inflorescences, a proxy for number of seeds). These seeds then contribute to a fraction of the number of recruits (*b*) entering the population at time* t+1 *with a size* z_{t+1} *given by the size distribution of recruits function* c*.*

s *= survival,* g *= growth (and shrinkage),* h *= flowering probability,* o *= reproductive effort per flowering event,* b *= recruitment rate,* c *= recruit size distribution.*

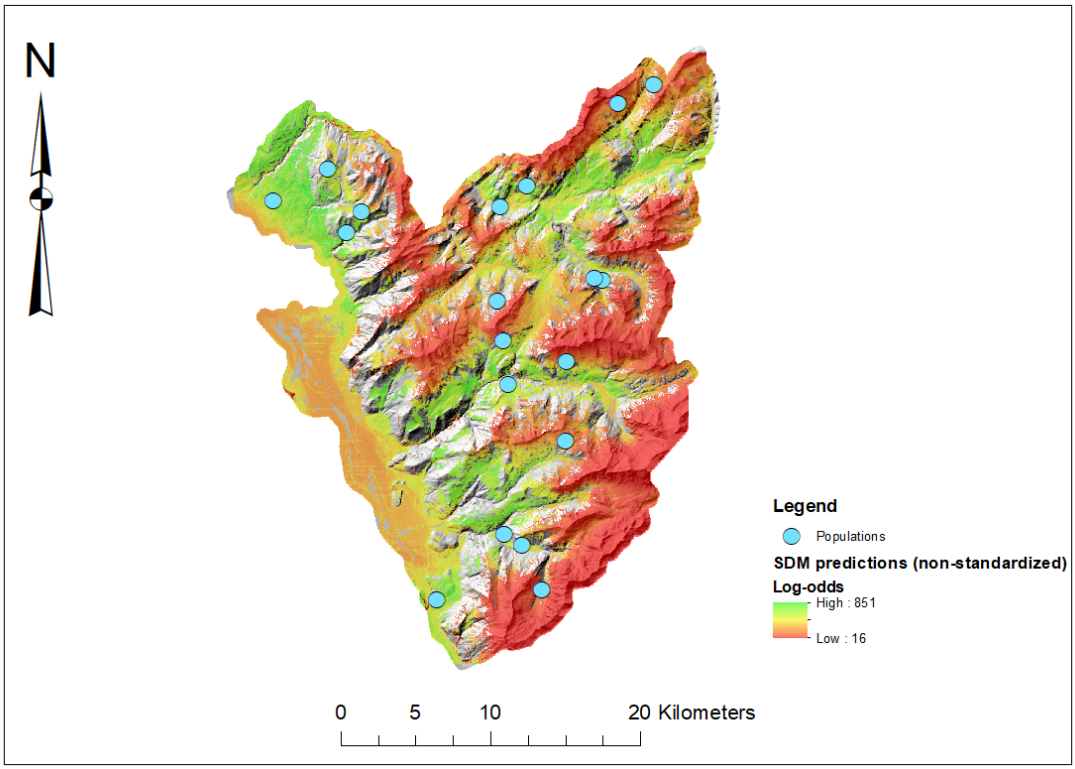

Figure S2.2.2 Geographic projection of the predicted environmental suitability on the study area. *Colour code represents the predictions of the weighted ensemble model (GBM, GLM and RF) in log odds.*

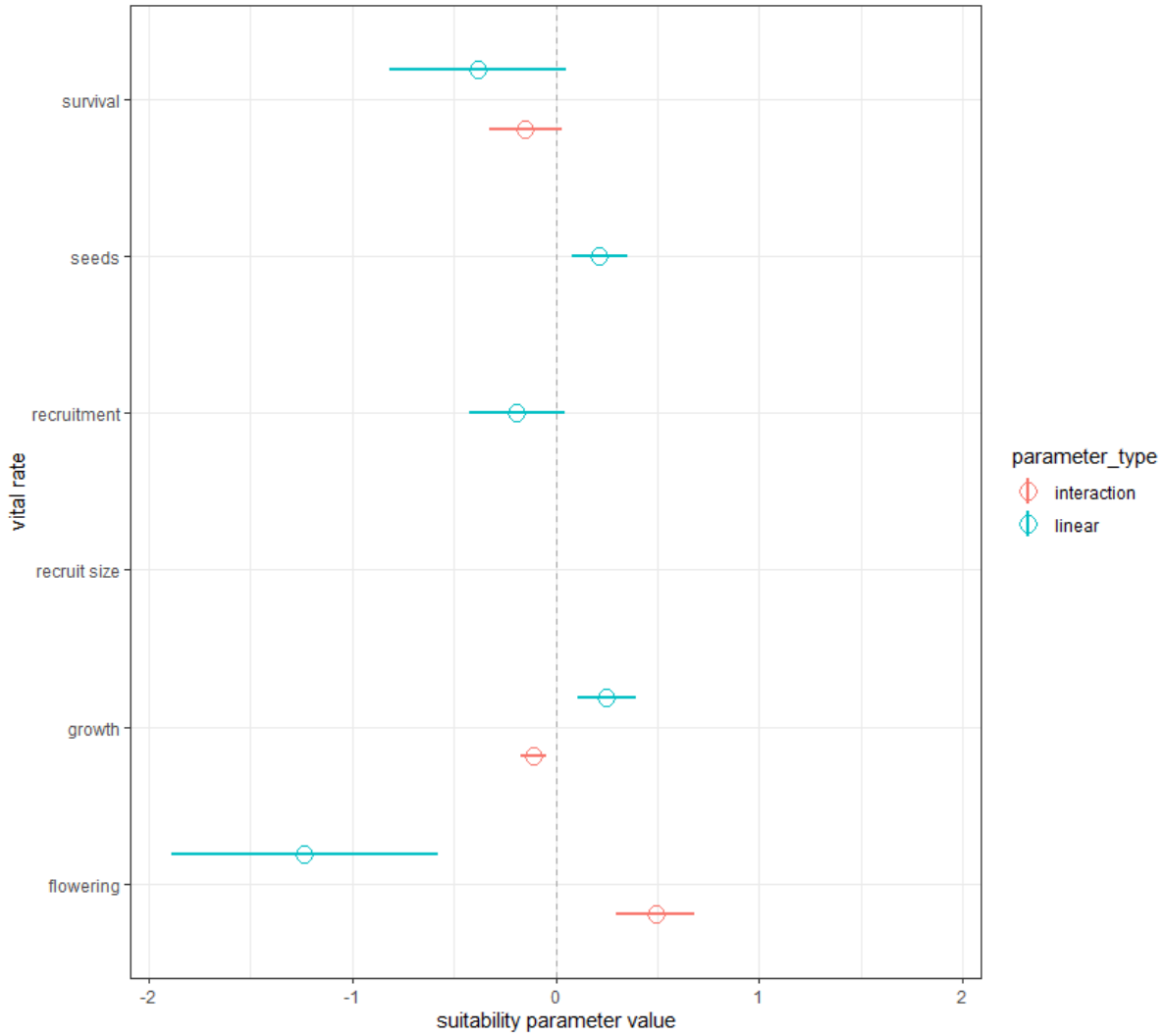

Figure S2.2.3: Summary of the effect of suitability on the different vital rates*. Vital rates are presented on the y-axis. Open circles represent the parameters for suitability in each vital rate model (x-axis), horizontal bars their 95% confidence intervals. Turquoise = linear term of the relationship between suitability and the vital rate, red = interaction between suitability and size to explain the vital rate. An absence of point means no term at all was maintained in the model.*

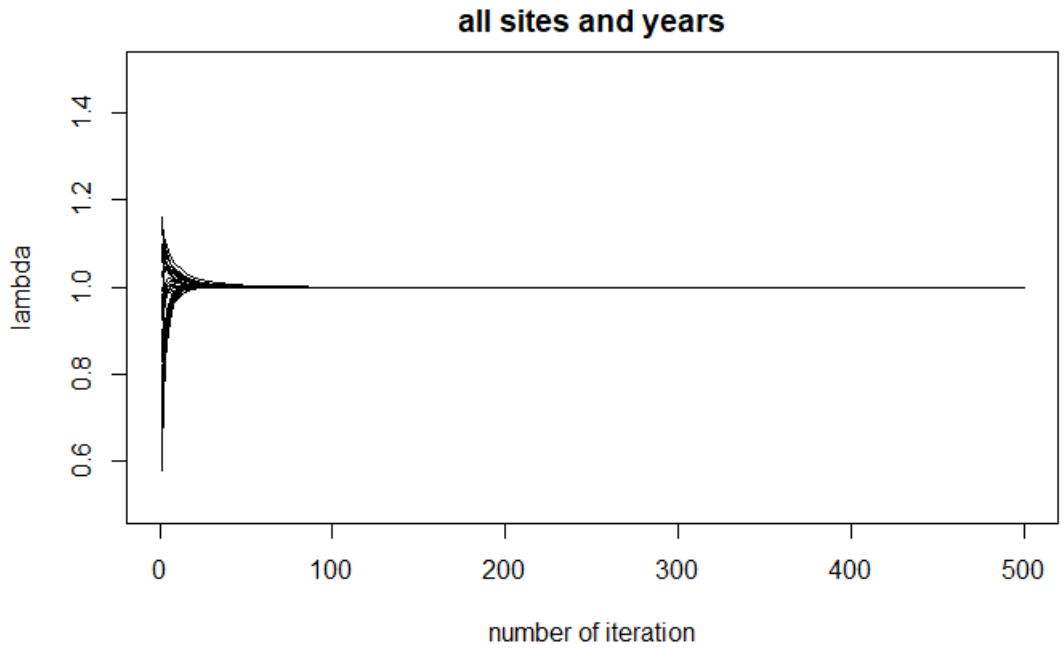

Figure S2.2.4 Convergence of the population growth rate as the population model is iterated towards equilibrium. *The x-axis shows the number of iterations: as our matrix model is based on an annual transition period, the number of iterations can be understood as equivalent to years. The y-axis shows the rate of increase of the population (population size at time t / population size at time t+1) as predicted by the model. Each line is based on the observations of one population in one transition.*

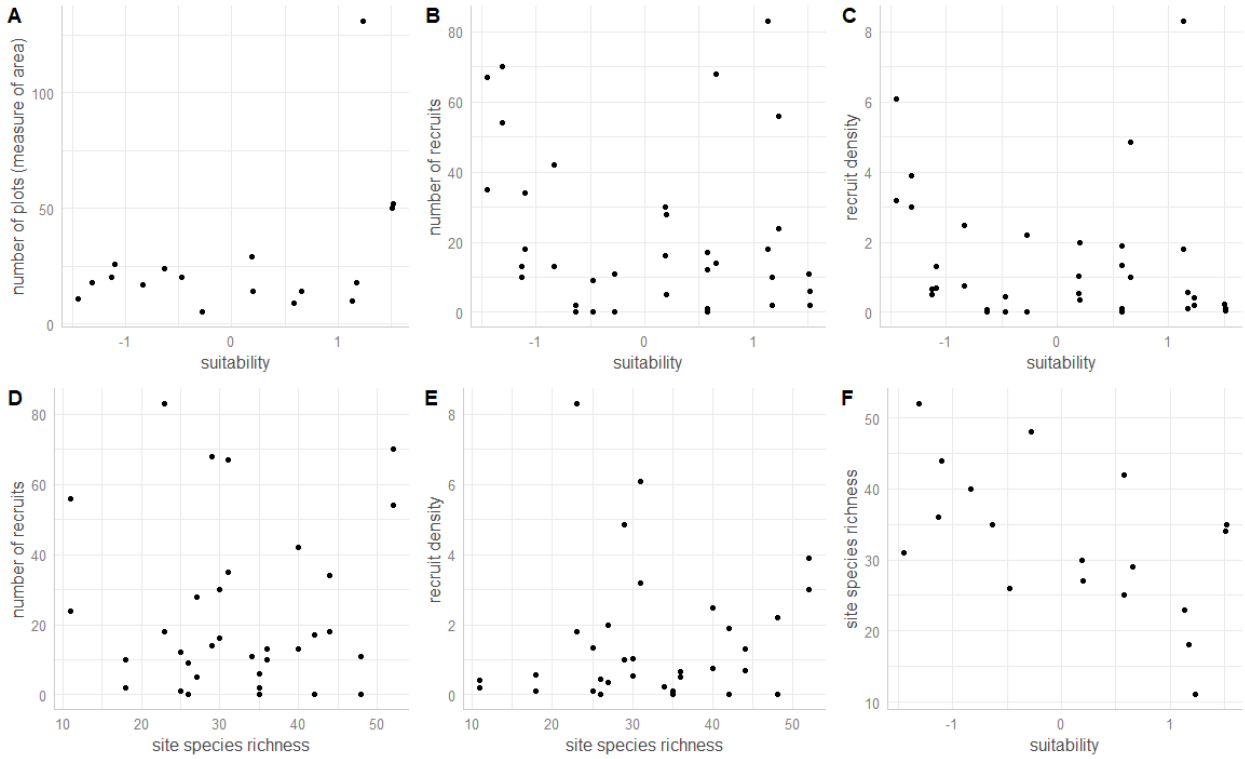

Figure S2.2.5 Plot of the raw data of useful information on recruits density. Upper part = components of recruit density*, with (A) area covered by each population, (B) number of recruits, (C) recruit density. One observation = one site****. Lower part = relationship with site species richness****, with (D) number of recruits and (E) recruit density over number of species. The number of species was inventoried in a 2m x 2m vegetation plot at the end of the demographic transects. Species were identified as best as possible to species or genus level, and some unidentified species were recorded as such. One observation = one site in one year. (F) relationship between species richness and environmental suitability. One observation = one site.*

Supplement S2.3: relationship between seed number and inflorescence length

In the Summer of 2019, inflorescences were collected at the field sites, around the monitored populations. These inflorescences were not collected not yet fully ripe, so that the seeds had not yet dispersed. The inflorescence length was measured, and the seeds were extracted from each inflorescence and counted. Some sites had to be revisited outside peak flowering season to obtain biological samples, and no seeds could be found in three sites.

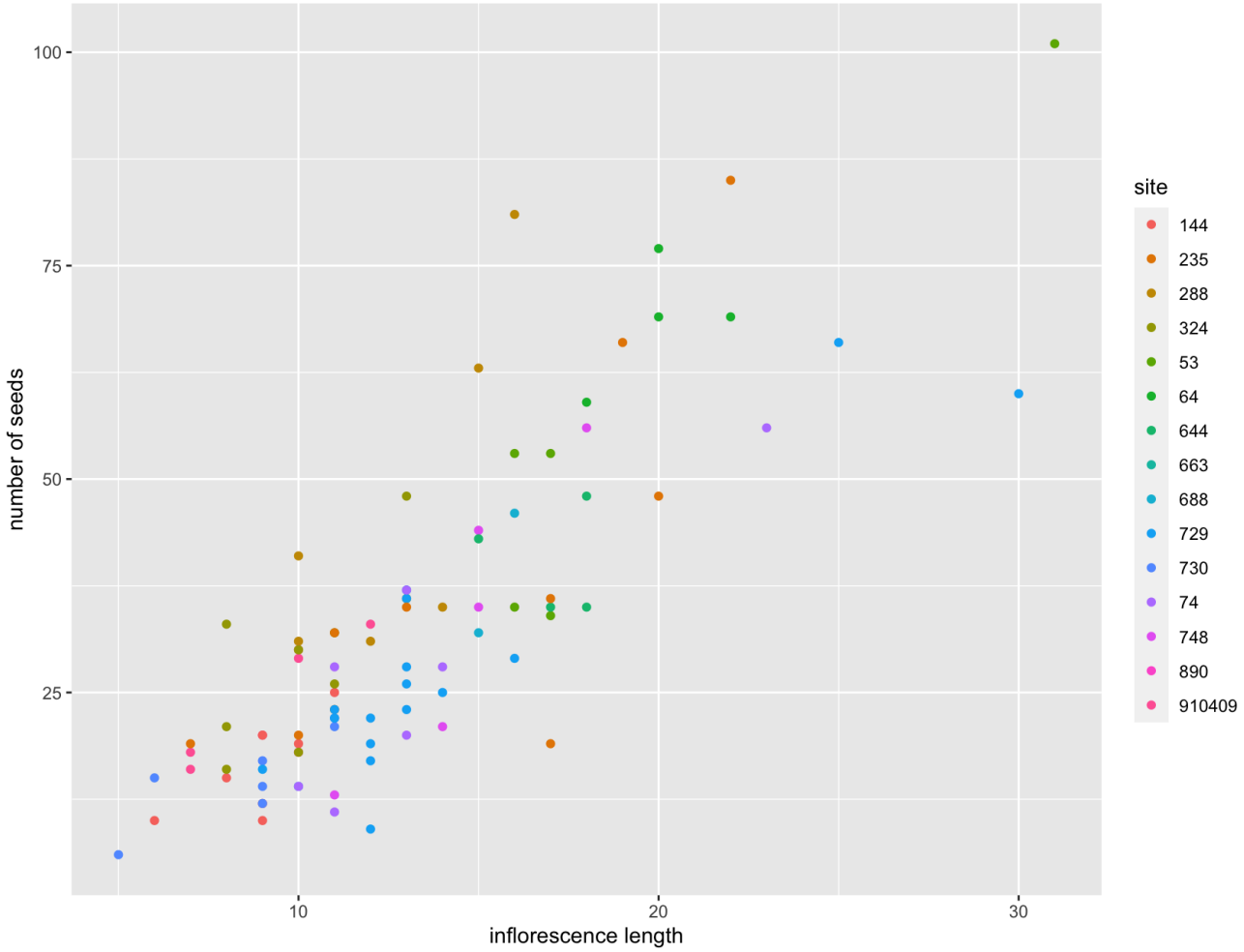

Figure S2.3.1 Relationship between the number of seeds per inflorescence and the length of the inflorescence *in fifteen sites from our study. The inflorescence length is measured in millimeters, and the relationships are for one inflorescence per plant only.*

From the gathered information, the relationship between number of seeds and inflorescence length was studied. We first display the raw data per site (Figure S4.1). We also built a generalized linear mixed model explaining the number of seeds as a function of the inflorescent length, with the site of origin as a random factor (intercept only). The number of seeds was modelled as Poisson distributed with a log link, using the lme4 package in R (Bates et al. 2015). The relationship between seed number and inflorescence length once adjusted for the correlation between samples stemming from the same sites is displayed in Figure S4.2.

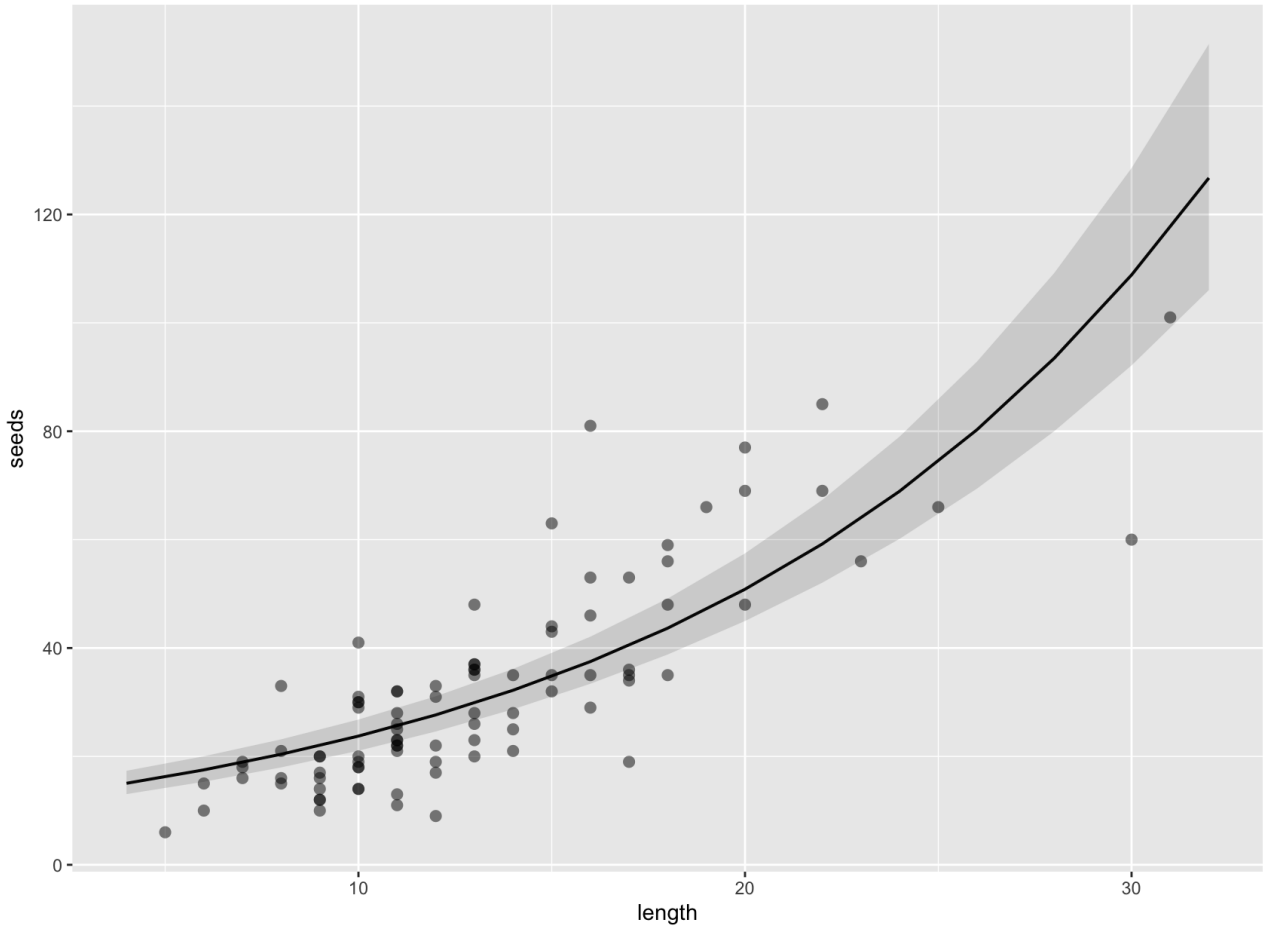

Figure S2.3.2 Modelled relationship between the number of seeds per inflorescence and the length of the inflorescence once the effect of sites has been accounted for. *The inflorescence length is measured in millimeters. The predicted line and confidence intervals stem from a generalized linear mixed model explaining the number of seeds as a function of inflorescence length as a Poisson distributed process (with log link), with the site of origin as a random intercept.*

Supplement S2.4 Supplementary Tables

Table S2.4.1 Model selection tables of the vital rates models

Detail of the model selection outputs on the vital rates models. The tables show candidate models for the selection.

*Size Y0 means size at time t, "^2" indicates a quadratic term, and size*suitability is the interaction between size at time t and suitability.*

*The columns for Intercept, size Y0, size Y^2 if applicable, suitability, suitability^2, transition, size*suitability indicate the parameter estimates for the fixed effect predictors, with NA meaning this predictor is not included in this candidate. dAICc is the delta AICc* (Bartoń 2018; Burnham and Anderson 2002)*: a difference in dAICc of less than two between two models means they have equivalent fit.*

Table S2.4.1.A survival

	Intercept	size Y0	suitability	suitability^2	transition	size * suitability	family	degrees of freedom	log likelihood	AICc	dAICc
1	0.14	0.97	-0.42	0.34	+	-0.15	binomial(logit)	8	-1518.39	3052.83	0.00
4	0.48	0.97	-0.38	NA	+	-0.15	binomial(logit)	7	-1519.63	3053.29	0.46
2	0.24	0.91	-0.65	0.33	+	NA	binomial(logit)	7	-1519.72	3053.47	0.64
3	0.55	0.91	-0.61	NA	+	NA	binomial(logit)	6	-1520.86	3053.74	0.91
5	0.50	0.91	NA	NA	+	NA	binomial(logit)	5	-1525.78	3061.57	8.74

Table S2.4.1.B growth

	Intercept (cond)	Intercept (disp)	size Y0	suitability	suitability^2	transition	size * suitability	family	degrees of freedom	log likelihood	AICc	dAICc
2	0.74	+	0.60	0.25	NA	+	-0.11	nbinom2(log)	12	-7865.41	15754.92	0.00
1	0.75	+	0.60	0.25	-0.01	+	-0.11	nbinom2(log)	13	-7865.39	15756.90	1.98
5	0.76	+	0.59	NA	NA	+	NA	nbinom2(log)	10	-7870.13	15760.33	5.41
4	0.76	+	0.59	0.04	NA	+	NA	nbinom2(log)	11	-7869.87	15761.83	6.91
3	0.77	+	0.59	0.04	-0.01	+	NA	nbinom2(log)	12	-7869.84	15763.78	8.86

Table S2.4.1.C flowering probability

	Intercept	size Y0	size^2	suitability	transition	size * suitability	suitability^2	family	degrees of freedom	log likelihood	AICc	dAICc
3	-7.91	4.36	-0.66	-1.23	+	0.49	NA	binomial(logit)	8	-1171.39	2358.82	0.00
7	-8.30	4.34	-0.66	-1.27	+	0.49	0.42	binomial(logit)	9	-1170.61	2359.27	0.45
2	-7.13	3.59	-0.48	NA	+	NA	NA	binomial(logit)	6	-1184.83	2381.68	22.86
1	-7.11	3.59	-0.48	-0.20	+	NA	NA	binomial(logit)	7	-1184.53	2383.09	24.27
4	-5.10	1.52	NA	-0.83	+	0.30	NA	binomial(logit)	7	-1190.04	2394.12	35.30
8	-5.55	1.51	NA	-0.87	+	0.29	0.46	binomial(logit)	8	-1189.06	2394.16	35.34
6	-5.09	1.52	NA	NA	+	NA	NA	binomial(logit)	5	-1196.28	2402.58	43.76
9	-5.57	1.52	NA	-0.28	+	NA	0.51	binomial(logit)	7	-1194.75	2403.52	44.70
5	-5.08	1.52	NA	-0.21	+	NA	NA	binomial(logit)	6	-1195.94	2403.91	45.09

Table S2.4.1.D reproductive effort

	Intercept	size Y0	suitability	suitability^2	transition	size * suitability	family	degrees of freedom	log likelihood	AICc	dAICc
3	2.09	0.44	0.22	NA	+	NA	gaussian(identity)	7	-481.20	976.67	0.00
2	2.05	0.44	0.22	0.03	+	NA	gaussian(identity)	8	-481.15	978.66	1.98
4	2.09	0.44	0.22	NA	+	0	gaussian(identity)	8	-481.20	978.75	2.08
1	2.05	0.44	0.22	0.03	+	0	gaussian(identity)	9	-481.15	980.75	4.07
5	2.06	0.46	NA	NA	+	NA	gaussian(identity)	6	-485.00	982.21	5.54

Table S2.4.1.E size of recruits

	Intercept (cond)	Intercept (disp)	suitability	suitability^2	transition	family	degrees of freedom	log likelihood	AICc	dAICc
3	0.68	+	NA	NA	+	nbinom2(log)	5	-1911.04	3832.14	0.00
2	0.68	+	0.13	NA	+	nbinom2(log)	6	-1910.03	3832.15	0.02
1	0.60	+	0.13	0.07	+	nbinom2(log)	7	-1909.85	3833.82	1.68

Table S 2: **Vital rates models and functions used to populate the matrix model. A) Vital rates models**, with the parameter estimates post model selection for the fixed effects. Random effects are indicated by terms in b: terms starting in $b0$ are random effects on the intercepts, terms starting in $b1$ are random effects on linear terms. The exact value of random effects (BLUP) varies depending on the site or plot and we hence summarize this by giving the distribution from which the estimates are drawn for each random effect included in our models. Note the flowering model (h) was fitted with optimx in lme4 as one of the default optimizers produced a convergence warning. **B) Density functions** used to predict population size distributions based on the vital rates equations. All other functions predict the mean value of the presented models for an individual of size z from a site w in transition T with the effect of suitability ϖ (functions $s(z_t,\varpi)$,$h(z_t,\varpi)$,$o(z_t,\varpi)$), or for site w with the effect of suitability ϖ (function $b(\varpi)$). Functions $s(z_t,\varpi)$,$h(z_t,\varpi)$ and $o(z_t,\varpi)$ predict for an average plot (u), i.e. only the random effects $b0_w$ and $b1_w$ are included in the predictions. The predictions are used to populate the matrices **S**,**G**,**P**,**F**,**H** and **O**

Panel A

Rate	Response	Link	Error	Model equation	Random structure	correlation	R^2c	R^2m
s	$P(survival)$	Logit	$E_{w,u,i}$ ~$binomial$	$(0.48 + b0_u + b0_w - 0.50_T) + (0.97)ln(z) - 0.38\varpi + -0.15ln(z)\varpi + E_{w,u,i}$	$b0_u$~$N(0,0.42)$ $b0_w$~$N(0,0.43)$	NA	0.33	0.16
g	z_i	log	$E_{w,u,i}$~neg binomial($\mu_1,\sigma_1 =$ 8.31)	$(0.74 + b0_u + b0_w + 0.23_T) + (0.6 + b1_u + b1_w)ln(z) + 0.25\varpi - 0.11\varpi ln(z) + E_{w,u,i}$	$b0_u$~$N(0,0.16)$ $b0_w$~$N(0,0.06)$ $b1_u$~$N(0,0.04)$ $b1_w$~$N(0,0.01)$	$\begin{array}{cc} & b1_u \quad b1_w \\ b0_u & \\ b0_w & \end{array}\begin{pmatrix} -0.91 & \\ & -0.77 \end{pmatrix}$	0.51	0.35
h	$P(flowering)$	logit	$E_{w,u,i}$~$binomial$	$(-8 + b0_u + b0_w + 0.19_T) + (4.36)ln(z) - 1.23\varpi - 0.66ln(z)^2 + 0.5\varpi ln(z) + E_{w,u,i}$	$b0_u$~$N(0,0.36)$ $b0_w$~$N(0,1.1)$	NA	0.49	0.26
o	$log(reproductive\ effort)$	Identity	$E_{w,u,i}$ ~$gaussian$	$(2.09 + b0_u + b0_w - 0.004_T) + (0.44)ln(z) + 0.22\varpi + E_{w,u,i}$	$b0_u$~$N(0,0.06)$ $b0_w$~$N(0,0.05)$	NA	0.37	0.24
c	$z_i - 2$	Log	$E_{w,u,i}$~neg binomial($\mu_2,\sigma_2 =$ 2.58)	$(0.68 + b0_u + b0_w + 0.15_T) + E_{w,i}$	$b0_u$~$N(0,0.18)$ $b0_w$~$N(0,0.12)$	NA	0.33	0.01
b	$\sqrt{\frac{r_w}{a_w}}$	Identity	E_w~$gaussian$	$0.96 - 0.19\varpi + E_{w,u,i}$	NA	NA	NA	0.07

Panel B

Density function	Equation	Terms definition
Adult genet size density function	$P(z_{t+1})$ =neg. binomial(mean= μ_1,dispersion parameter= σ_1)	where μ_1 is the prediction of model g and σ_1 is the dispersion parameter of model g
Recruits size density function	For $z_{t+1} > 1$, $P(z_{t+1})$ =neg. binomial(mean= μ_2,dispersion parameter= σ_2) For $z_t + 1 < 2$, $P(z_{t+1}) = 0$ as the minimal size in our model is 2 leaved individuals	where μ_2 is the prediction of model c and σ_2 is the dispersion parameter of model c

Supplement S2.5 Detail of the recruitment model selection

Several candidate recruitment models (*b*) were attempted, for different density dependence scenarios: compensatory density dependence, density independent and constant recruitment. Detail of the models are given in equations 4, 5 and 6.

As the studied populations have different densities, and the PlantPopNet protocol monitors as many 50 x 50 cm plots necessary to sample 100 individual genets in the first year of fieldwork, we fitted our candidate recruitment models on the number of recruits per plot (r_w/a_w) in any site *w* via generalized least squared (gls). The use of gls was necessary to compare linear and non-linear response curves. The use of the number of recruits per unit area is necessary to have comparable, meaningful densities to study the effects of density dependence. The response variable was square root transformed to normalize the residuals and yield a more homogeneous variance of the error in all candidate models.

Our density independent model is described in equation 4. In this model, every unit of reproductive effort linearly produces a proportion (p_0) of the number of recruits.

$$\frac{r_w}{a_w} = p_0 * \frac{o_w}{a_w} \qquad \textbf{equation 4}$$

where o_w is the sum of reproductive effort (mm of inflorescences) produced by all individuals in site w and a_w the number of plots (unit area) sampled at site w.

Our constant recruitment model is described in equation 5. It describes a scenario where only a certain number of microsites become available every year in any given population, constraining the number of recruits entering the population the next year to a specific plateau value R_{max}.

$$\frac{r_w}{a_w} = R_{max} \qquad \textbf{equation 5}$$

Equation 6 assumes a compensatory density dependent process through a reparametrized Beverton-Holt equation where every unit of reproductive effort contributes linearly to the pool of recruits at low density, but at higher densities the probability of recruitment decreases up to a plateau value *Rmax* (Beverton & Holt, 1957: see supplementary material **S2.6** for the reparametrization).

$$\frac{r_w}{a_w} = \frac{p_0 * \left(\frac{o_w}{a_w}\right)}{1 + \frac{p_0 * \left(\frac{o_w}{a_w}\right)}{R_{max}}}$$ **equation 6**

We assumed that the parameters *p0* and *Rmax* could vary, or not, as a function of enviromental suitability such as detailed in equations 7-10.

$$p_0 = \beta_0 + \beta_1 \varpi$$ **equation 7**

$$R_{max} = \beta_2 + \beta_3 \varpi$$ **equation 8**

or

$$p_0 = \beta_0$$ **equation 9**

$$R_{max} = \beta_2$$ **equation 10**

We only let either *p0* or *Rmax* at a time to vary as a function of suitability in the Beverton-Holt model, to limit our models to three parameters to be estimated on the basis of 36 non-independent observations (2 observations of 18 sites).

This led us to a total of seven candidate recruitment models. These seven candidate recruitment models were then compared using AICc values. The recruitment models were fitted via generalized least squares using the nlme package (Pinheiro et al., 2020). AICc values were determined using the MuMIn package (Bartoń, 2018). The results of the AICc based model comparison are presented in **Table S2.5.1.**

There was a wide range of existing densities in our observed populations, such that the number of 0.25m^2 plots that needed to be sampled to guarantee a population size of at least 100 individuals in the first year of the study varied between 4 and 127 (**Figure S2.5.1**, colour legend). The model that had the lowest AICc was the constant recruitment model with carrying capacity varying as a function of suitability (model C.1, **Table S2.5.1**). The constant recruitment model with no effect of suitability performed nearly as good in terms of AICc. We therefore selected model C.1, but note the potential impacts of this choice in the discussion. The prediction of a constant recruitment model, compared to those of a Beverton Holt model are displayed in **Figure S2.5.2**

Table S2.5.1 Results of the recruitment model selection. *The various models represent different regimes of density dependence. Column four ("Detail of the parameters and relationship to suitability") details the way environmental suitability was allowed to affect recruitment and density dependence in all models. The selection of the best model was performed based on AICc value, mode details on other metrics are available in supplement S1. Recruitment models were fitted via generalized least squares using the nlme package (Pinheiro et al., 2020). AICc values were determined using the MuMIn package (Bartoń, 2018).*

Model name	**Recruitement type**	**Equation**	**Detail of the parameters and relationship to suitability**	**AICc**
I.1	No density dependence	$\frac{r}{a} = p_0 * S$	$p_0 = \beta_0 + \beta_1 * \varpi$	103
I.0	No density independence		$p_0 = \beta_0$	104
BH.1.R	Compensatory density dependence	$\frac{r}{a} = \frac{p_0 * S}{1 + \frac{p_0 * S}{R_{max}}}$	$p_0 = \beta_0$ $R_{max} = \beta_1 + \beta_2 * \varpi$	90
BH.1.P	Compensatory density dependence		$p_0 = \beta_0 + \beta_1 * \varpi$ $R_{max} = \beta_2$	88
BH.0	Compensatory density dependence		$p_0 = \beta_0$ $R_{max} = \beta_1$	89
C.1	Constant recruitment	$\frac{r}{a} = R_{max}$	$R_{max} = \beta_0 + \beta_1 * \varpi$	81.8
C.0	Constant recruitment		$R_{max} = \beta_0$	82

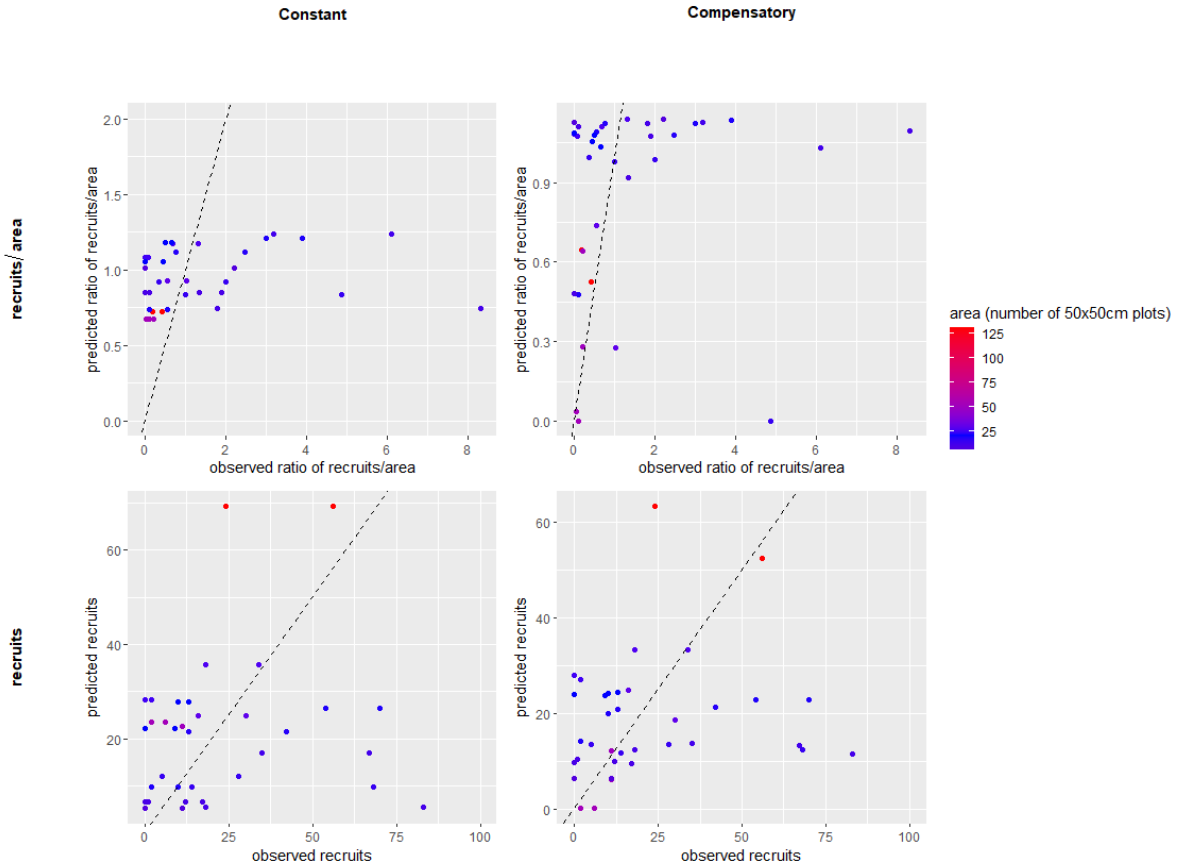

Figure S2.5.2 Details of predictions of two candidate recruitment models evaluated for this study. *Left panels show the results of the constant recruitment model (model C.1, see main text), while right hand panels show the results of the compensatory recruitment model for comparison (model BH.1.P, see main text). Upper panels are in the original scale of the models, i.e. in number of recruits per unit area (r/a, table 2 and equations 4-6) either observed (x-axis) or predicted (y-axis) at any given site. Lower panels are reported in actual number of recruits (r, table 2 and equations 4-6) either observed (x-axis) or predicted (y-axis) at any given site.*

Supplementary material S2.6: Reparametrization of the Beverton Holt Equation

Let's start with our Beverton Holt recruitment function (Beverton & Holt 1957), where R is the number of expected recruits per unit area, S is the number of stems per unit area, and b_0 and b_1 are the parameters:

$$R = \frac{S}{b_0 + b_1 S}$$

Define R_{max} as the asymptotic number of recruits. Divide numerator and denominator on the right hand side by S

$$R = \frac{1}{\frac{b_0}{S} + b_1}$$

and let S tend to ∞ :

$$R_{max} = lim_{S \to \infty} \frac{1}{\frac{b_0}{S} + b_1} = \frac{1}{b_1}$$

One can then rewrite the recruitment function in terms of asymptotic number of recruits:

$$R = \frac{S}{b_0 + \frac{S}{R_{max}}}$$

One can reparameterise this by setting $p_0 = 1/b_0$, which results in:

$$R = \frac{p_0 S}{1 + \frac{p_0 S}{R_{max}}}$$

The p_0 parameter turns out to be the slope of the recruitment function at $S = 0$, i.e. the proportion of seeds that recruit in the absence of density dependence. The parameters are now meaningful and can be directly compared to the parameters of the other two models we use in our study. Let p_0 get very big and you get to the constant recruitment model (equation 6, main text). Let R_max be very big and we obtain the density independent model (equation 5, main text).

Supplements to: Chapter 3 Intraspecific variation in functional traits and their demographic consequences along an environmental suitability gradient for a perennial herb

Added information on the SDM: see Supplementary material S2.1.1

In an attempt to reduce redundancy, this section is presented only once, in Chapter 2.

Supplement S3.1 Plots of the raw data and correlations between traits (if available)

S3.1.1 Correlations between predictors. *One observation = one site*

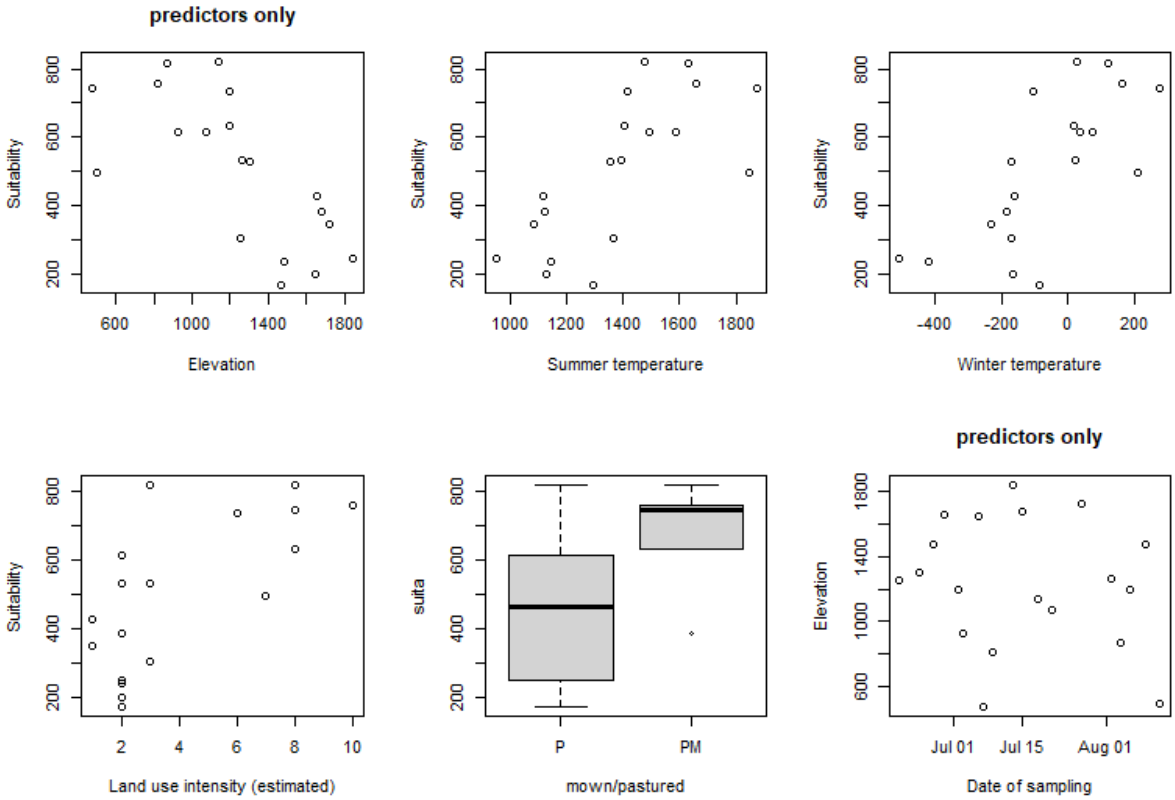

S3.1.2 Correlation between leaf traits. *One observation = one individual*

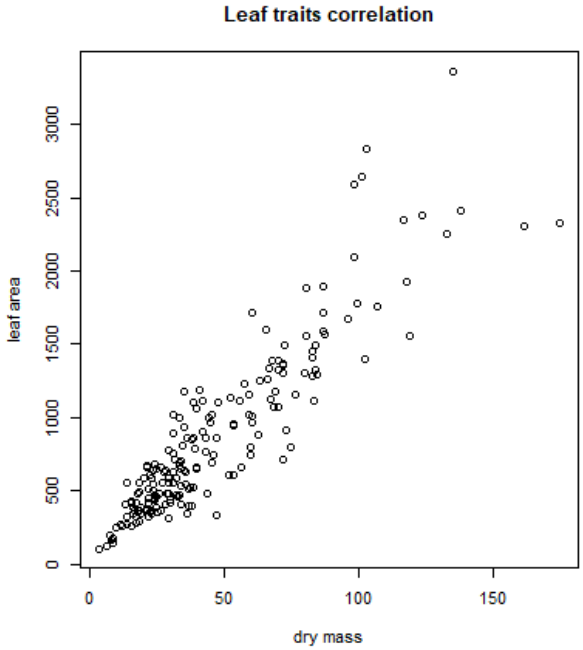

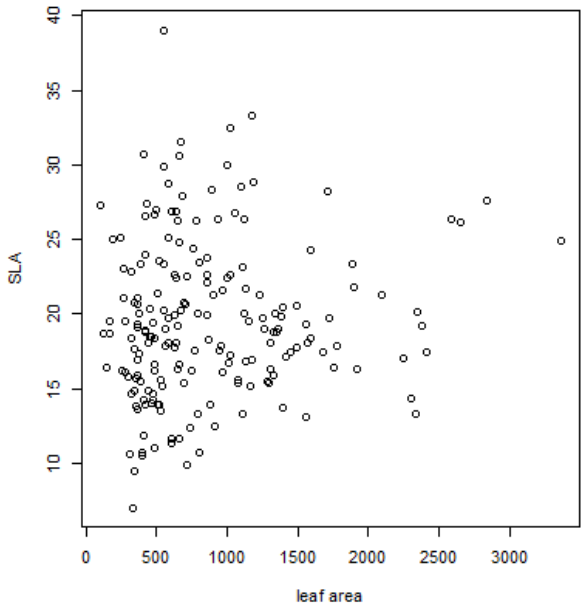

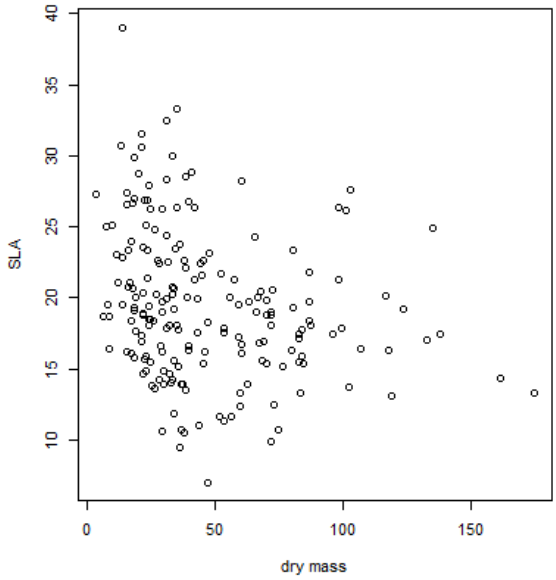

S3.1.3 Specific Leaf Area over predictors

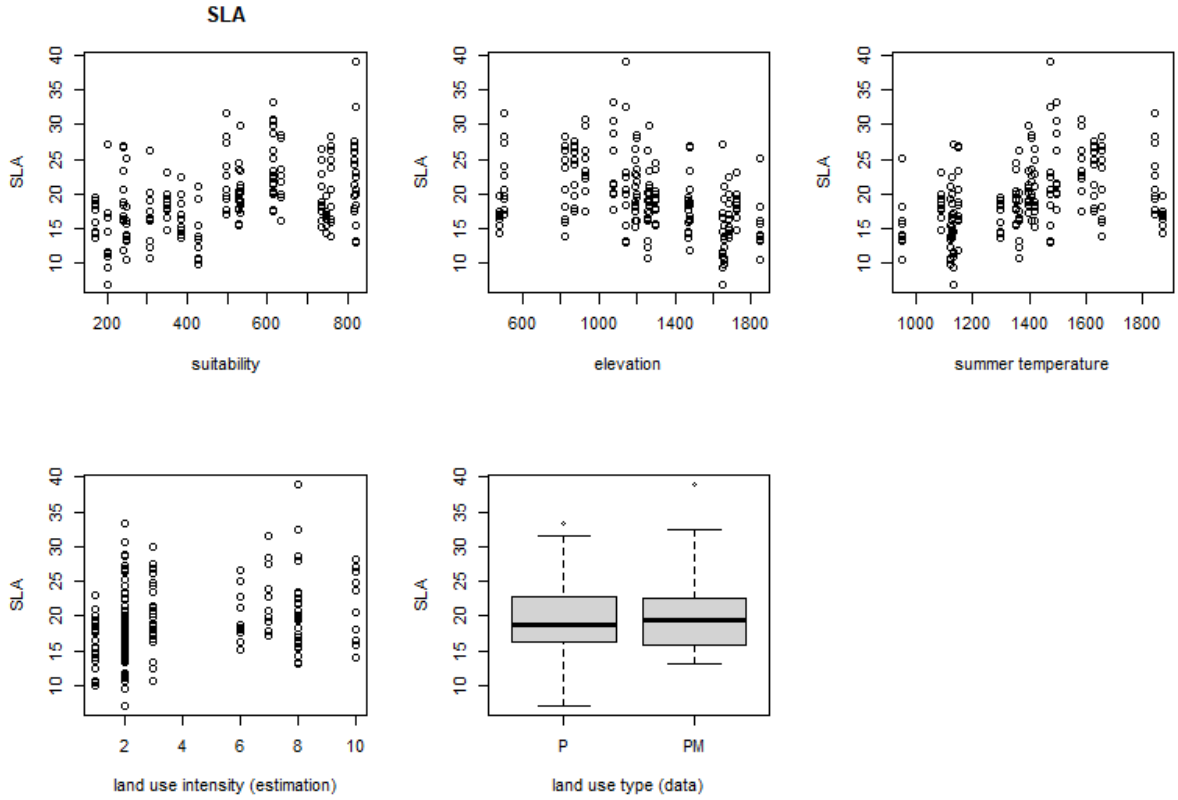

S3.1.4 Leaf Mass over predictors

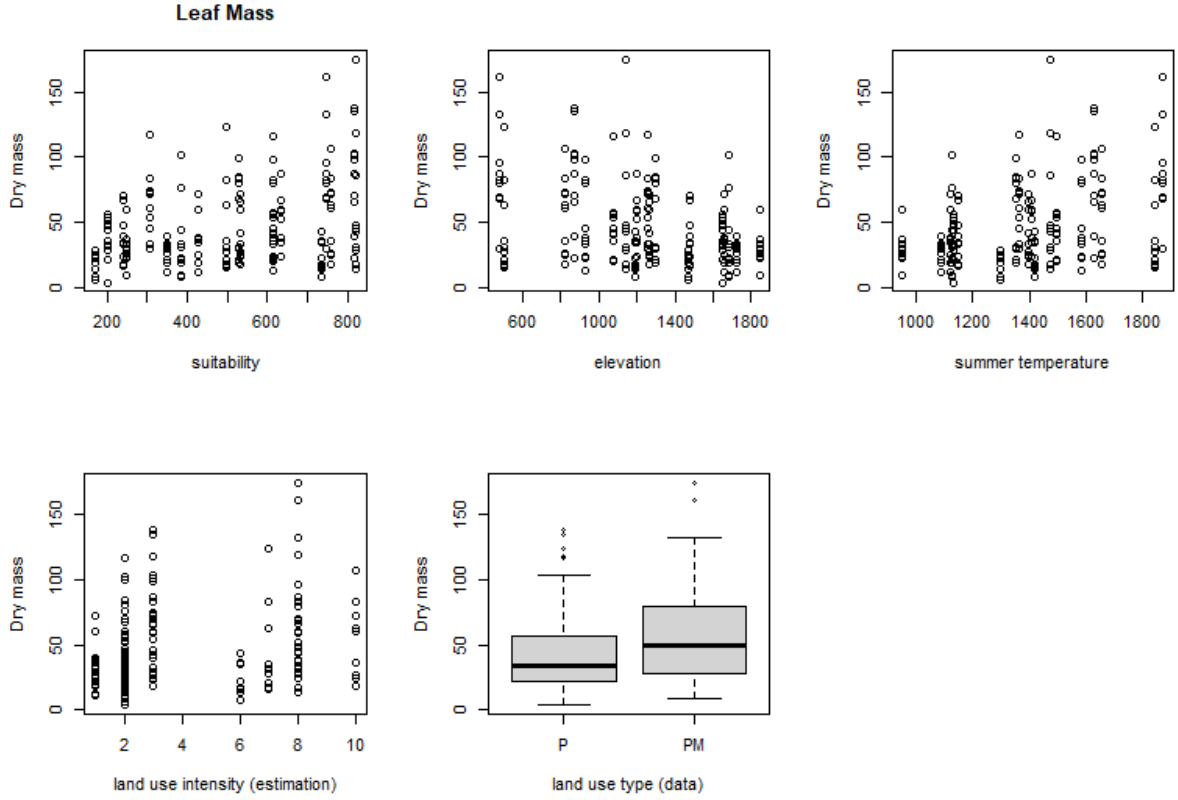

S3.1.4 Leaf Area over predictors

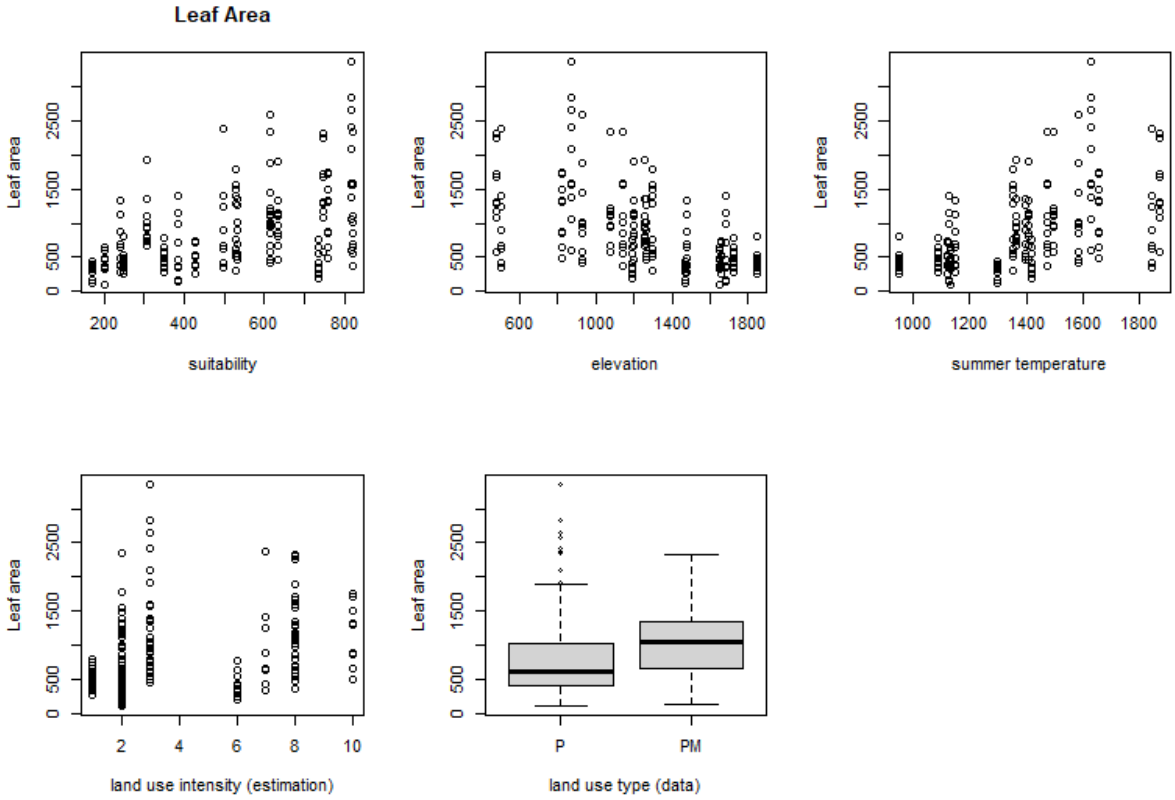

S3.1.1 Seed Mass. *One observation = average mass of one seed, on one inflorescence*

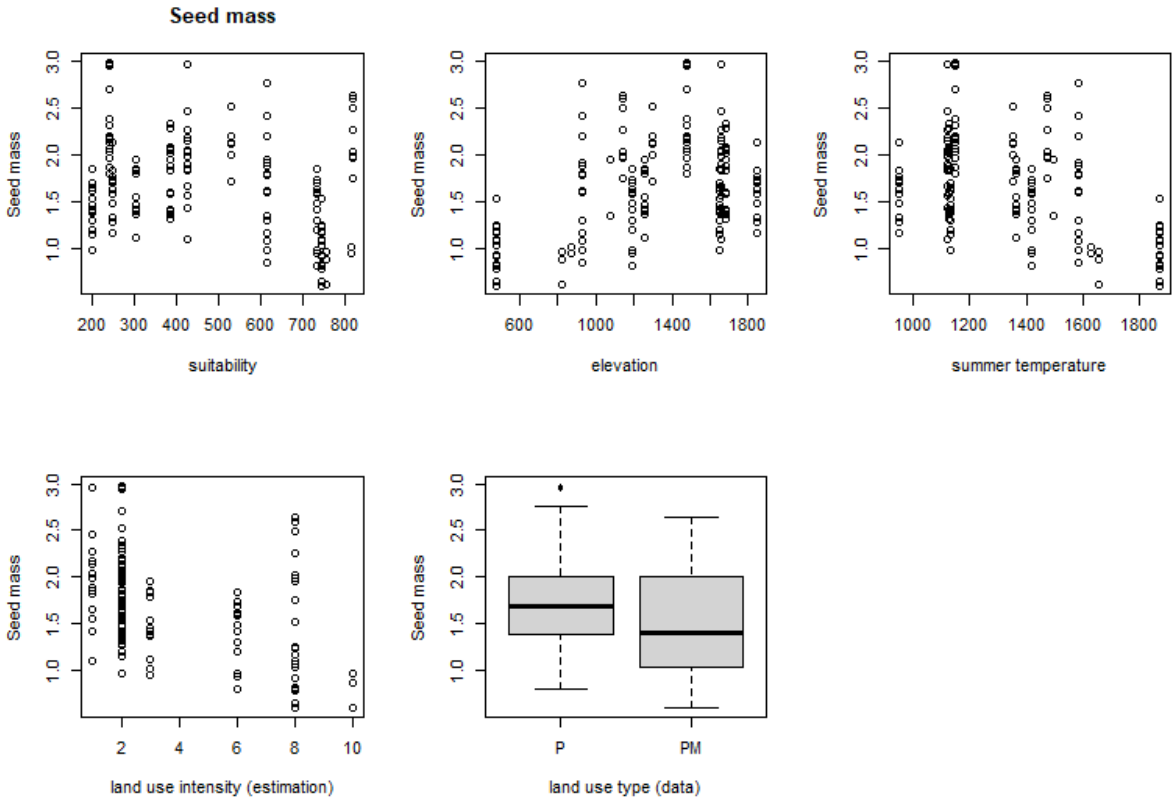

S3.1.1 Seed Number. *One observation = one inflorescence*

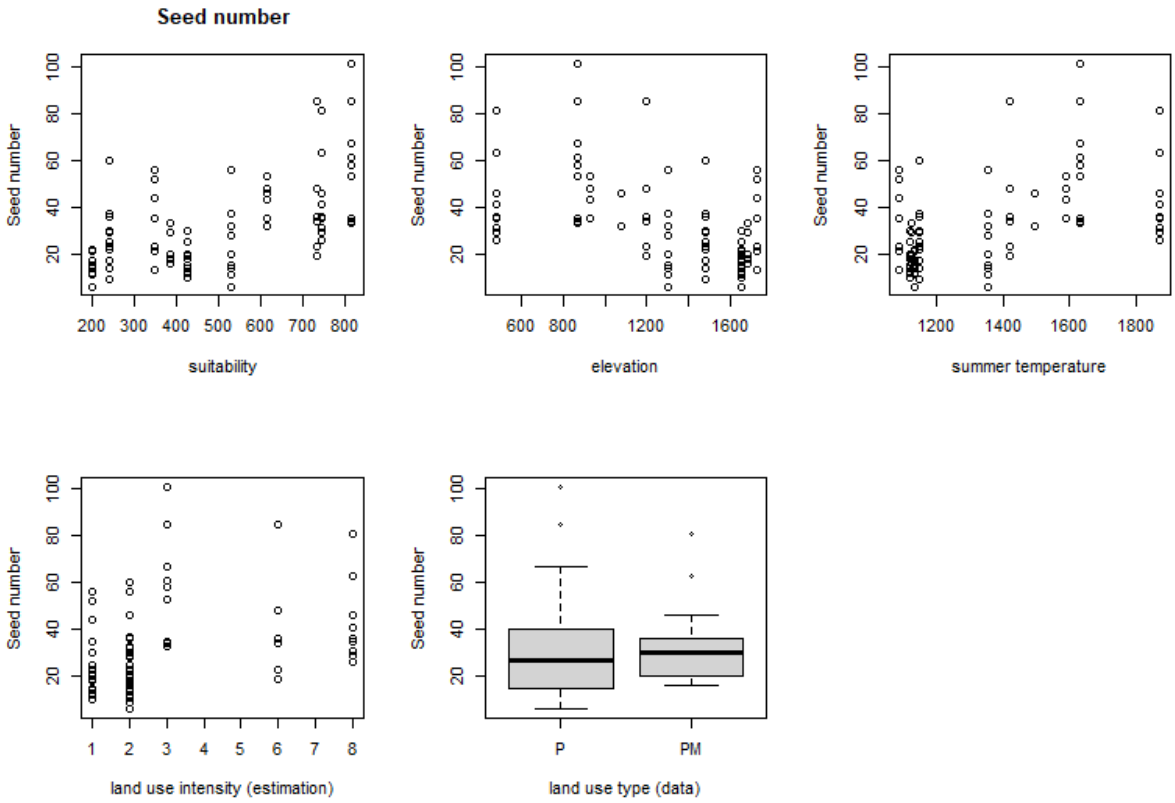
Seed number
Seed number
suitability
elevation
summer temperature
land use intensity (estimation)
land use type (data)
P
PM

Supplement S3.2 Details of the survival models

Table S3.2.1 Survival as a function of Leaf Area in interaction with suitability

MODEL INFO:
Observations: 4047
Dependent Variable: individual survival at time t + 1
Type: Mixed effects generalized linear regression
Error Distribution: binomial
Link function: logit

MODEL FIT:
AIC = 3764.17, BIC = 3808.31
Pseudo-R^2 (fixed effects) = 0.18
Pseudo-R^2 (total) = 0.35

FIXED EFFECTS:

	Est.	2.5%	97.5%	z val.
(Intercept)	2.96	2.56	3.36	14.54
LA	-0.45	-0.83	-0.07	-2.32
suitability	-0.34	-0.65	-0.02	-2.09
transition	-1.14	-1.32	-0.97	-12.67
LA:suitability	0.61	0.36	0.86	4.71

RANDOM EFFECTS:

Group	Parameter	Std. Dev.
plot	(Intercept)	0.88
site_code	(Intercept)	0.34

Grouping variables:

Group	# groups	ICC
plot	362	0.18
site_code	18	0.03

Table S3.2.2 Survival as a function of Leaf Area without interaction with suitability

MODEL INFO:
Observations: 4047
Dependent Variable: individual survival at time t + 1
Type: Mixed effects generalized linear regression
Error Distribution: binomial
Link function: logit

MODEL FIT:
AIC = 3779.97, BIC = 3811.49
Pseudo-R^2 (fixed effects) = 0.08
Pseudo-R^2 (total) = 0.35

FIXED EFFECTS:

	Est.	2.5%	97.5%	z val.
(Intercept)	3.35	2.86	3.84	13.41
LA	-0.33	-0.70	0.05	-1.69
transition	-1.14	-1.32	-0.97	-12.69

RANDOM EFFECTS:

Group	Parameter	Std. Dev.
plot	(Intercept)	0.87
site_code	(Intercept)	0.76

Grouping variables:

Group	# groups	ICC
plot	362	0.16
site_code	18	0.13

Table S3.2.3 Survival as a function of Specific Leaf Area in interaction with suitability

MODEL INFO:
Observations: 4047
Dependent Variable: individual survival at time t + 1
Type: Mixed effects generalized linear regression
Error Distribution: binomial
Link function: logit

MODEL FIT:
AIC = 3768.58, BIC = 3812.72
Pseudo-R^2 (fixed effects) = 0.16
Pseudo-R^2 (total) = 0.35

FIXED EFFECTS:

	Est.	2.5%	97.5%	z val.
(Intercept)	3.01	2.57	3.45	13.27
SLA	-0.43	-0.77	-0.08	-2.42
suitability	-0.24	-0.57	0.09	-1.42
transition	-1.14	-1.32	-0.97	-12.70
SLA:suitability	0.55	0.21	0.89	3.14

RANDOM EFFECTS:

Group	Parameter	Std. Dev.
plot	(Intercept)	0.87
site_code	(Intercept)	0.43

Grouping variables:

Group	# groups	ICC
plot	362	0.18
site_code	18	0.04

Table S3.2.4 Survival as a function of Specific Leaf Area without interaction with suitability

MODEL INFO:
Observations: 4047
Dependent Variable: individual survival at time t + 1
Type: Mixed effects generalized linear regression
Error Distribution: binomial
Link function: logit

MODEL FIT:
AIC = 3774.05, BIC = 3805.58
Pseudo-R^2 (fixed effects) = 0.12
Pseudo-R^2 (total) = 0.35

FIXED EFFECTS:

	Est.	2.5%	97.5%	z val.
(Intercept)	3.36	2.91	3.81	14.73
SLA	-0.55	-0.89	-0.22	-3.24
transition	-1.14	-1.32	-0.97	-12.69

RANDOM EFFECTS:

Group	Parameter	Std. Dev.
plot	(Intercept)	0.87
site_code	(Intercept)	0.63

Grouping variables:

Group	# groups	ICC
plot	362	0.17
site_code	18	0.09

Summary tables printed with use of the jtools package (Long 2020).

Supplement S3.3 Relationship between functional traits and elevation

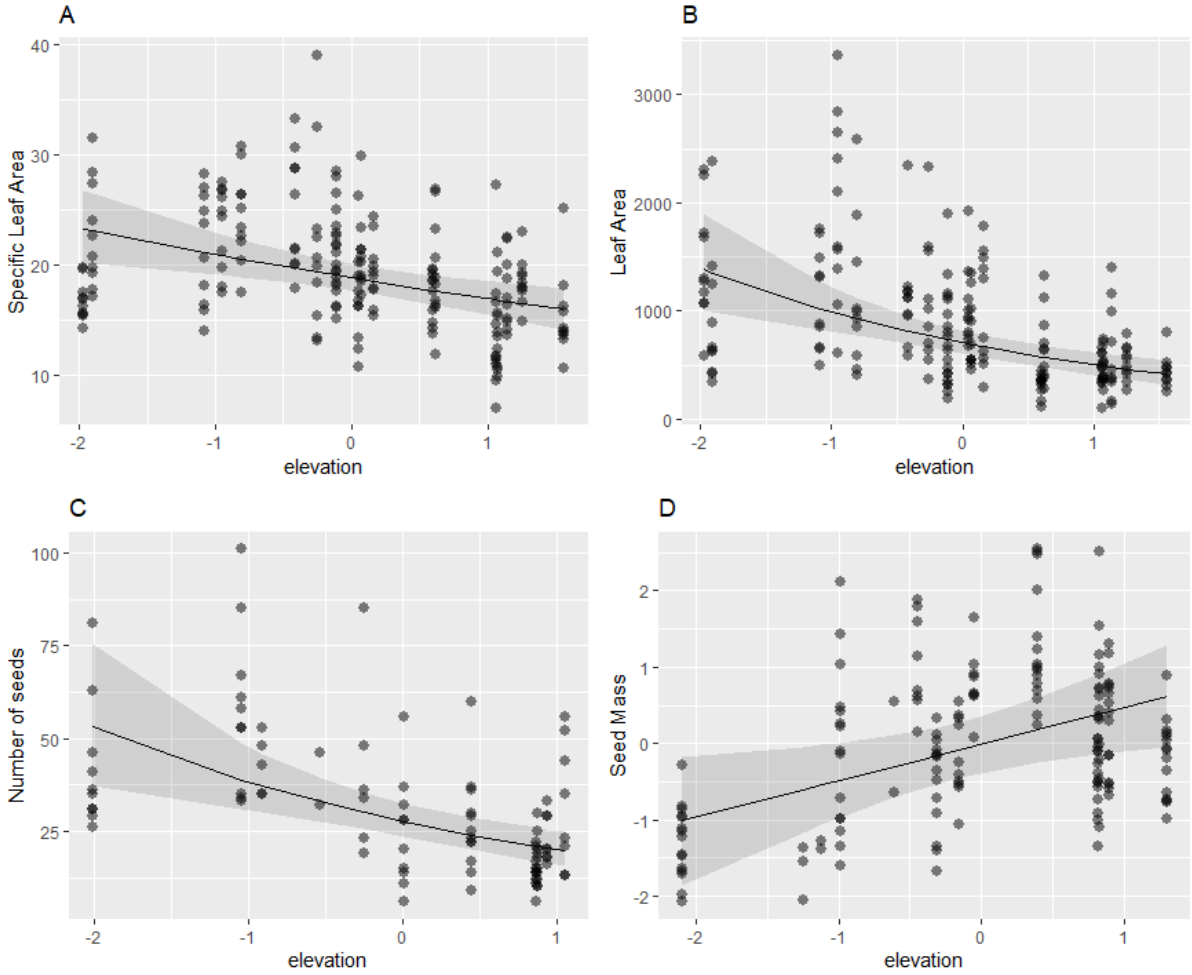

Figure S3.3.1 Relationship between elevation and functional traits: A) SLA, B) LA, C) Number of seeds per inflorescence D) seed mass. *The prediction line and 95% confidence intervals stem from a linear mixed model with suitability as a fixed effect and site as a random effect. Suitability is the mean standardized output of the Species Distribution Model.*

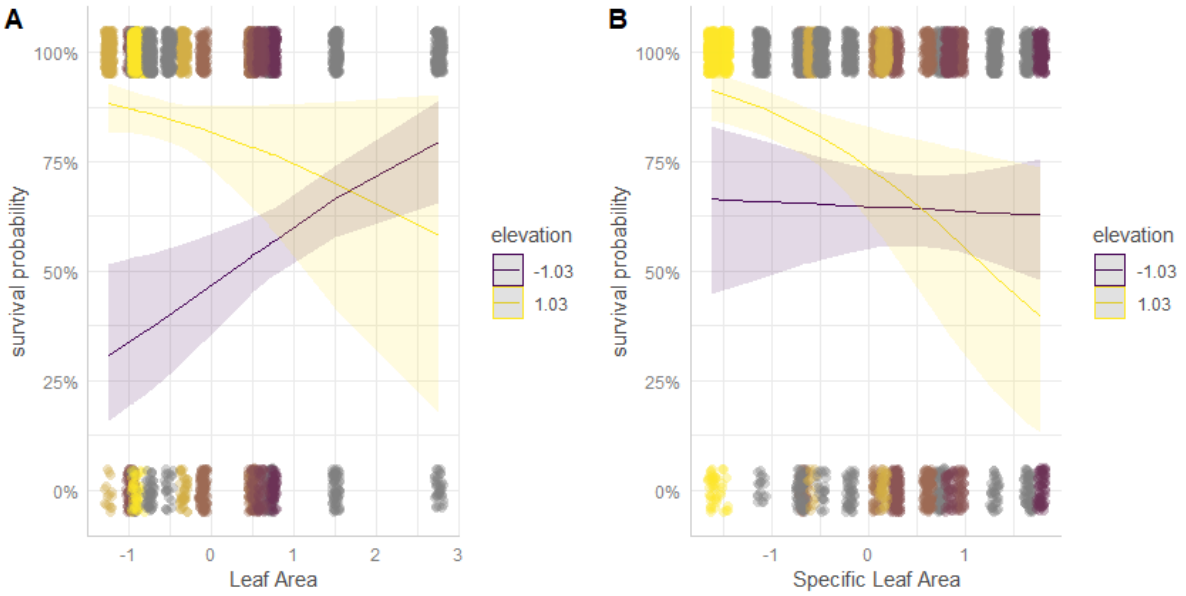

Figure S3.3.1 Relationship between LA (A) or SLA (B) on survival in interaction with elevation. *Panel A shows the relationship between LA (x-axis) and survival probability (y-axis). Panel B shows the relationship between SLA (x-axis) and survival probability (y-axis). The interaction between elevation and the functional trait in explaining survival is represented by the two colored lines, where deep purple shows the relationship at the lowest elevation where a population was monitored. Light yellow shows the relationship at the highest elevation. Points are coloured as per the lines. The shaded areas represent the 95% confidence interval for the predictions. Each observation is an individual from one of the 18 populations: points are shown with jitter to avoid overlap. Plots created using the ggeffects package* (Lüdecke 2018) *using the viridis colour-blind friendly colour maps* (Garnier et al. 2021).

Supplements to: Chapter 4 - Evidence for a slower life cycle in low SDM-predicted probability of occurrence areas in the perennial herb *Plantago lanceolata* L.

Supplement S4.1: Supplement to data sources

In this study, we focused on the first two transitions of the PlantPopNet database. We used the Y0_V1.02, Y1_V1.1. and Y2_V1.1 standard data products. In addition, we performed the following data cleaning and investigation steps. Population CDF was excluded as the number of individuals still alive (*i.e.*, the population excluding dead plants and new recruits) in Y1 did not match with the number of individuals in Y0 or Y2. A shift in columns for individuals 121 and 121 in population LK1 (LK1_T1_P8_121 and LK1_T1_P8_122) was detected and corrected (no leaves = NA, leaf length = 95, respectively 72 and leaf width = 6, respectively 28) and individual 8 in population SW242 (SW242_T2_P20_8) was deleted following an issue on tracking the rosettes between year 0 and y1.

Life cycle of the focal species: see Figure S2.2.1

In an attempt to reduce redundancy, this figure is presented only once, in Chapter 2.

Supplement S4.2 Variable importance in the two SDM approaches represented in the main text.

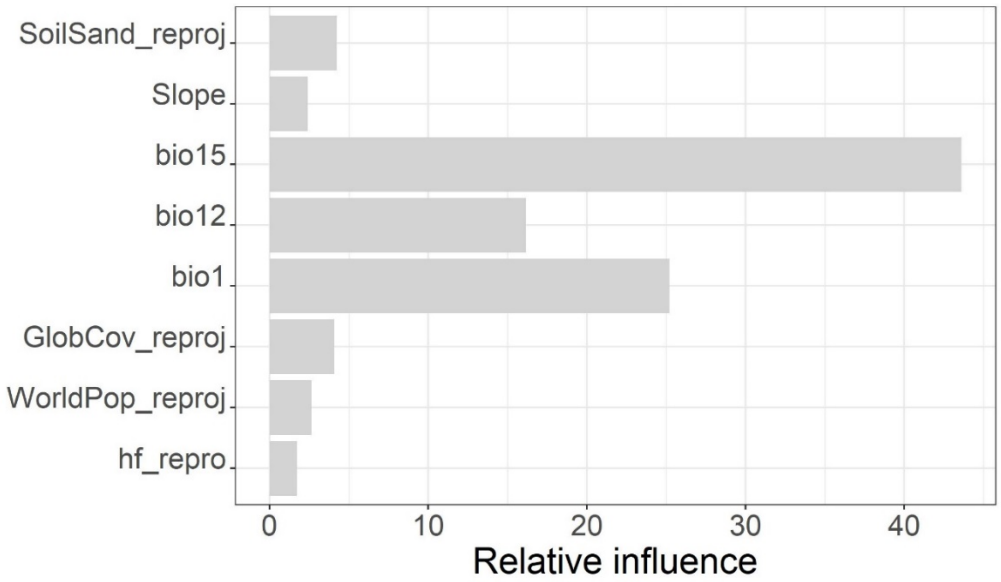

Figure S4.2.1 Relative influence of each environmental predictors in the species-specific SDM-approach. *The relative influence is computed as the squared error attributed to each variable in the random boosted regression tree technique applied for the species specific SDM (Elith et al. 2008; Greenwell et al. 2018)**.** Legend of layer's names: SoilSand_reproj = soil sand contents (proportion of sand), bio15 = precipitation seasonality, bio 12 = annual precipitation, bio 1 = mean annual temperature, GlobCov_reproj = global land use cover, WorldPop_reproj = population density, hf_repro = human footprint.*

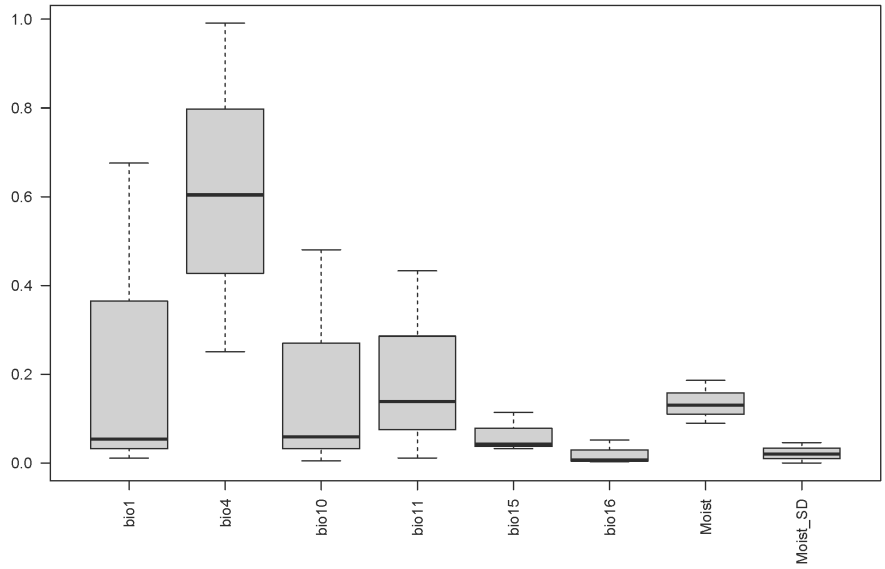

Supplement S4.2.2 Variable importance of each environmental predictors in the generic SDM. *The variable importance is a standardized metric of the mean importance of each variable across the different runs of the different algorithms included in the final ensemble model as a max-TSS weighted average* (Thuiller et al. 2016)***.*** *Legend of predictors' names: bio1 = mean annual temperature, bio 4 = temperature seasonality, bio 10 = mean temperature of the warmest quarter, bio 11 = mean temperature of the coldest quarter, bio 15 = precipitation seasonality, bio 16 = precipitation of the wettest quarter, moist = annual potential evapo-transpiration, moist_SD = seasonality of the annual potential evapo-transpiration.*

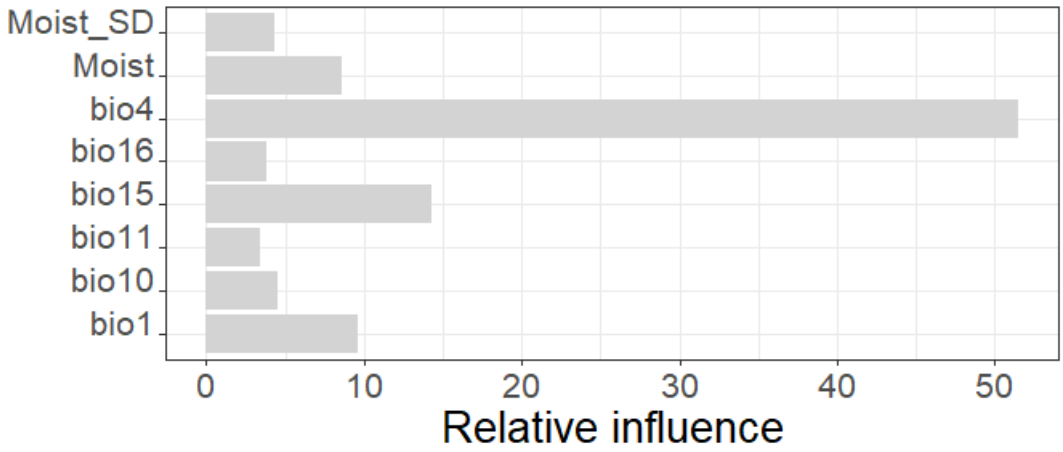

Supplement S4.2.3 Relative influence of each environmental variable when the species specific-SDM approach is applied on the generic SDM predictors (Hybrid approach 1, Supplement S4.3). *The relative influence is computed as the squared error attributed to each variable in the random boosted regression tree technique applied for the species specific SDM* (Elith et al. 2008; Greenwell et al. 2018)***.*** *Legend of predictors' names: bio1 = mean annual temperature, bio 4 = temperature seasonality, bio 10 = mean temperature of the warmest quarter, bio 11 = mean temperature of the coldest quarter, bio 15 = precipitation seasonality, bio 16 = precipitation of the wettest quarter, moist = annual potential evapo-transpiration, moist_SD = seasonality of the annual potential evapo-transpiration.*

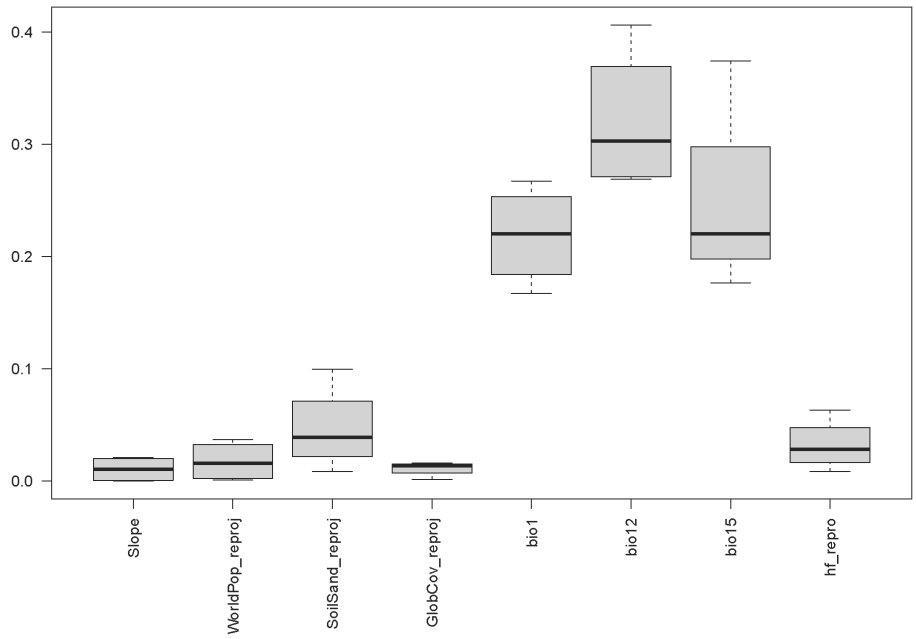

Supplement S4.2.4 Variable importance of each environmental predictors when the generic SDM approach is applied on the species-specific environmental predictor (Hybrid approach 2, Supplement S4.3). *The variable importance is a standardized metric of the mean importance of each variable across the different runs of the different algorithms included in the final ensemble model as a max-TSS weighted average* (Thuiller et al. 2016)*. Legend of layer's names: SoilSand_reproj = soil sand contents (proportion of sand), bio15 = precipitation seasonality, bio 12 = annual precipitation, bio 1 = mean annual temperature, GlobCov_reproj = global land use cover, WorldPop_reproj = population density, hf_repro = human footprint.*

Supplement S4.3 Consequences of a swap of predictors between SDM-approaches.

As the relationships between life history strategies (LHS) and environmental suitability as predicted by a Species Distribution Model (SDM-suitability) were so distinct between the two Species Distribution Models (SDM), we performed a reciprocal swap between predictors of the two modelling techniques. We performed the generic SDM-approach using the environmental predictors from the species-specific SDM approach (hybrid 1: Figure S4.3.1). Vice versa, we performed the species-specific SDM modelling on the "classic" plant-SDM environmental predictors (Broennimann et al. 2007; Csergő et al. 2017; Petitpierre et al. 2012; Thuiller et al. 2005). We will call this second swap hybrid 2 (Figure S4.3.2 and S4.3.3). Our expectation was that the environmental predictors of the species-specific SDM would produce the same trends in demography in both techniques, and that the environmental predictors of the generic SDM would fail to detect meaningful trends in both techniques. We expected each SDM approach to have better evaluation metrics when applied on the species specific environmental predictors. We expected the generic SDM approach to always yield better evaluations, as it uses repeated split sampling rather than spatial blocks for the cross validation. Results are displayed and discussed hereafter.

The generic SDM method with specific predictors (hybrid 1) had excellent evaluation metrics, with Kappa = 0.84, max-TSS = 0.832 and AUC = 0.969. Overall, the average trends of the Generic-SDM with the species-specific predictors were similar to those of the original GBM approach, but the confidence intervals were broader (Figure S4.3.1, compared to Figure 4.4, main text).

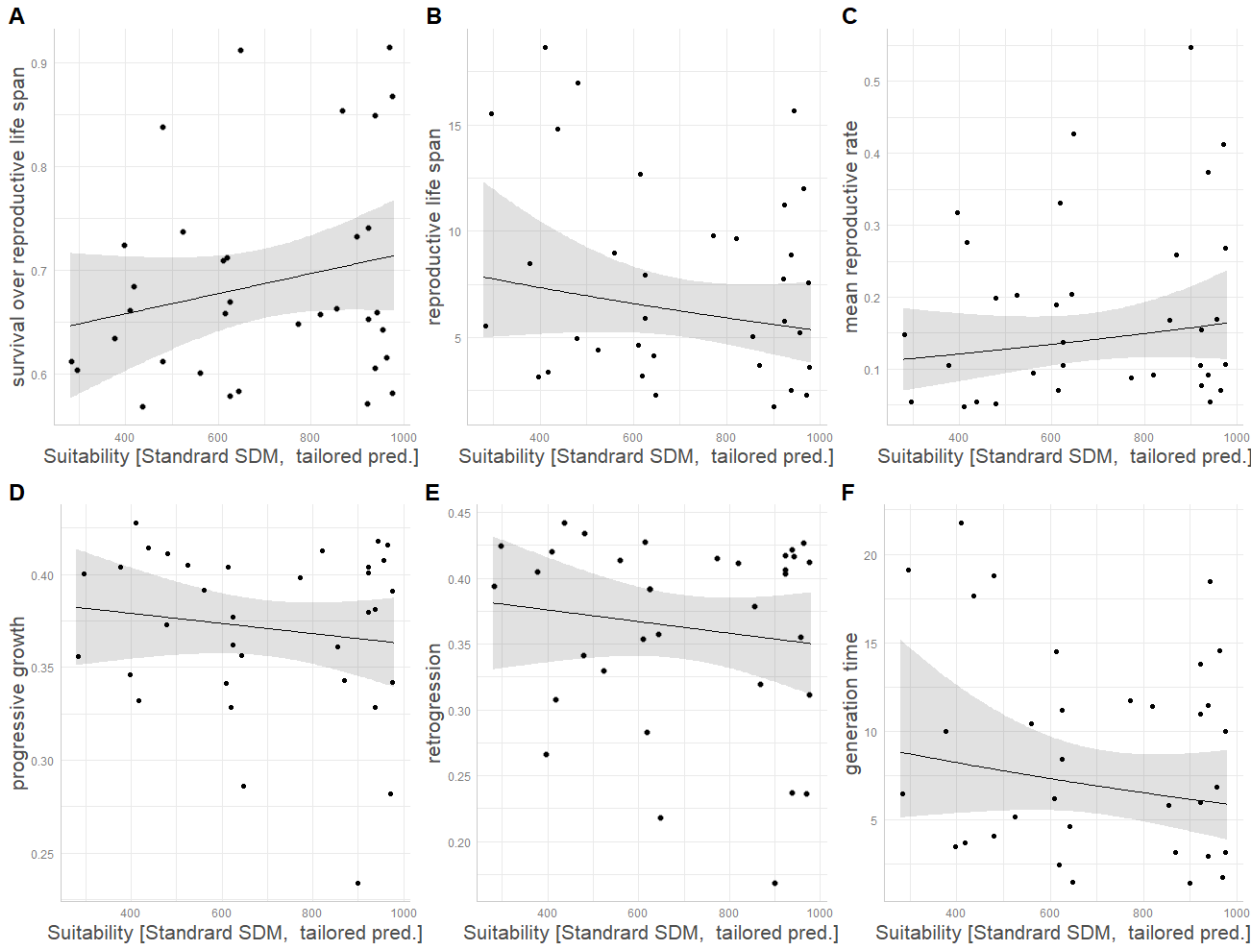

Figure S4.3.1 Speed of the life cycle over the SDM-predicted suitability for P. lanceolata, when the generic-SDM procedure is applied using the species-specific predictors [Hybrid 1]. *Black lines and shaded areas are the predictions and 95% confidence interval of a linear model predicting each life history metric as a function of SDM-suitability. Reproductive life expectancy, mean yearly reproduction, generation time were log transformed in the models. One observation = one PlantPopNet population (time averaged).*

When applying the species-specific modelling approach on the classic SDM predictors (hybrid 2), a methodological modification had to be performed. The number of spatial blocks had to be decreased to 2 when using this set of predictors, based on the results of the spatialAutoRange analysis in BlockCV (Valavi et al. 2019). The performance metrics were high: Kappa = 0.78, max-TSS = 0.78, AUC = 0.95, but over only two spatial blocks, which makes it not directly comparable to the 5-spatial block result on the species-specific environmental predictors. The demographic over suitability models supported a quadratic relationship between LHS and SDM-suitability Figure S4.3.2). If a straight relationship was

fitted, trends similar as when using the species specific predictors emerged, but much weaker (Figure S4.3.3, compared to Figure 4.4, main text).

Discussion

The consequences of our swap in environmental predictors between the two SDM approaches seems to indicate several important results. First, the generic SDM-approach can capture the same trends in demographic strategies when applied on the species specific predictors. Nonetheless, the trends are not as clear, and the evaluation metrics of the SDM

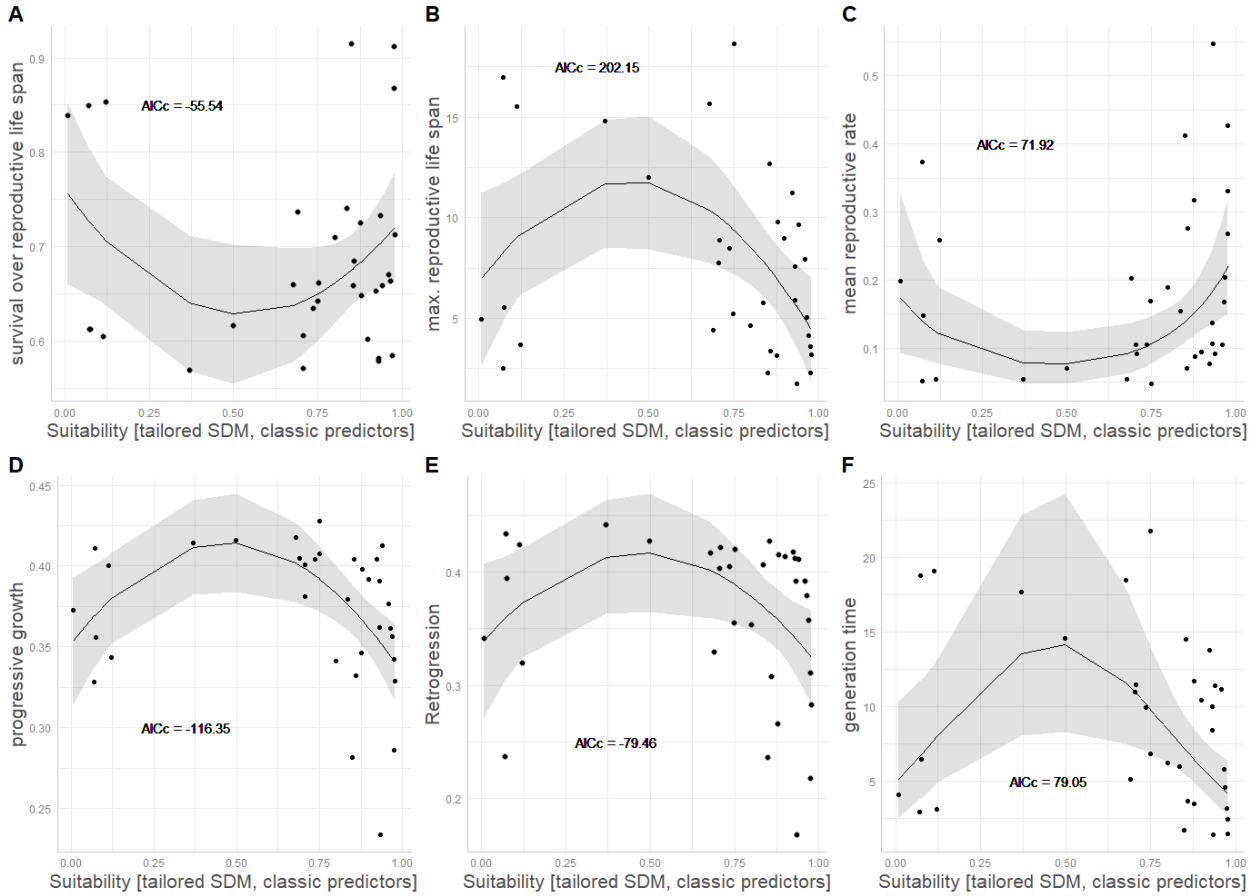

Figure S4.3.2: Speed of the life cycle over the SDM-predicted suitability for P. lanceolata, when the species specific-SDM approach is applied using the classic predictors. *The AICc values of models supposing a quadratic relationship between LHS and suitability were lower than for a linear model (see Figure S2.3). The AICc values are displayed in each panel* (Bartoń 2018).

itself are not as high as with the original predictors. The results of the species-specific SDM applied on classic environmental predictors (hybrid 2) are harder to interpret. The evaluation metrics of this SDM were higher than the original species-specific SDM, but this is probably due to the fact that only two spatial blocks could be used in the spatial block cross validation. A spatial block cross validation uses data from another geographic area to validate the model, making it harder to obtain good evaluation metrics than with a repeated split sampling (where the dataset is randomly separated in two parts, with 70% of the data being used for model calibration and 30%, randomly selected from any geographic area, for model evaluation). The number and size of the blocks is chosen based on the spatial correlation of

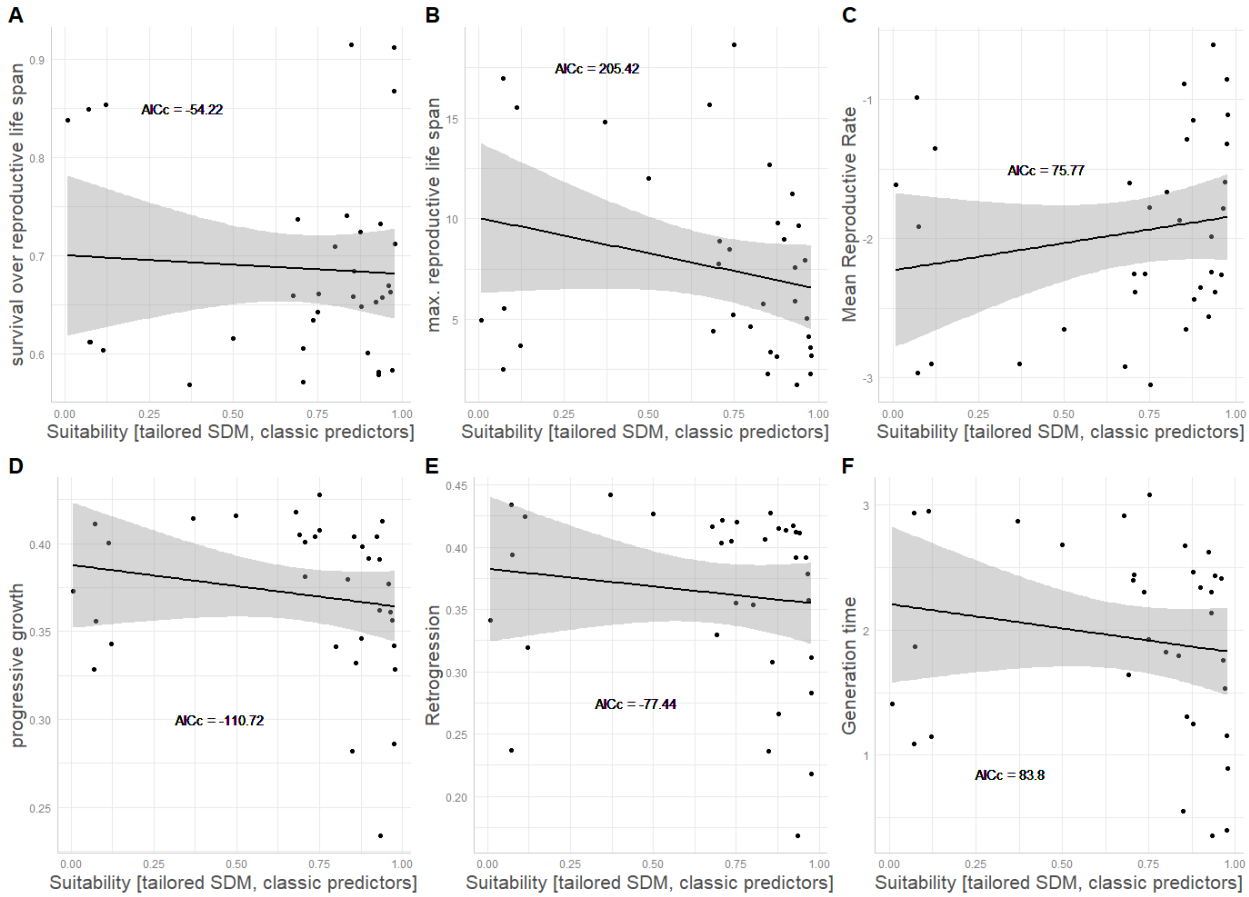

Figure S4.3.3: Speed of the life cycle over the SDM-predicted suitability for P. lanceolata, when the species specific-SDM approach is applied using the classic predictors, and when the relationship between Life History Strategy metrics and suitability is forced to be linear. *The AICc values are displayed in each panel* (Bartoń 2018).

predictors in space (Roberts et al. 2017; Valavi et al. 2019). With the original species-specific environmental predictors, five spatial blocks were selected, making it harder to obtain good evaluation metrics.

Then, the relationships between demography and suitability as predicted by our hybrid 2 are hard to interpret. A quadratic relationship between LHS and suitability was supported by our LHS over suitability models (Figure S4.3.2). Quadratic relationships are common in ecology, with optima at intermediate values of an environmental driver and conditions decreasing in optimality on both sides of that optimum (Begon, Townsend, and Harper 2006). There is very little theoretical support for a quadratic relationship between overall demographic performance and probability of occurrence. Indeed, the expectation is that a decreasing environmental optimality on both sides of an environmental gradient would result in a decreasing probability of occurrence (see for instance (Maguire, 1973). Rather, we take this quadratic trend to be an effect of the lack of information at the middle range of suitability values, and the difficulty to fit any meaningful trend in these SDM-suitability to LHS models. Indeed, the confidence interval of the linear models are very broad (Figure S4.3.3).

Except for the probability of survival across the reproductive life, slopes are similar to those detected with the original species- specific SDM (though they could very well be flat), which is counter to our expectations. There is hence something further than the choice of environmental predictors to our species specific SDM that makes it capture the demographic trends we were expecting.

The generic SDM approach did not include interactions between predictors (Csergő et al. 2017). In comparison, we chose to use a random boosted regression tree as a fitting algorithm in our species specific SDM. We selected this approach as it made it possible to capture interactions between environmental predictors, without having to stipulate them a-priori (Elith et al. 2008). Random boosted regression trees are a machine learning technique which will create repeated splits of the data based on the values of the provided predictors. It will split the data multiple times, based on which predictor can explain the most variance at the current split. As a consequence, any interaction or any for and between any predictors can be easily captured. It is likely that there were interactions between predictors that could

not be captured by several of the algorithms used in the ensemble model forming our Generic-SDM approach. This is supported by the fact that a preliminary model excluding the Maxent algorithm (another machine learning technique that could capture interactions included in the Generic-SDM approach (Phillips, Anderson, and Schapire 2006) provided flatter and more uncertain relationships between SDM-suitability and Life History Strategy Metrics (not shown).

One last point to these technical considerations is the overall evaluation metrics of the SDM. The best SDM in terms of Kappa, max-TSS and AUC remains the generic-SDM approach, with Kappa = 0.849, Max-TSS = 0.857 and AUC = 0.983. This is part due to the use of a different cross validation strategy in the species-specific versus generic SDM approaches. The use of spatial block cross validation approach in our species-specific SDM makes it harder to obtain very high evaluation metrics. But the generic-SDM is an ensemble of algorithms, which includes a similar random boosted regression tree. This algorithm alone had evaluation metrics of Kappa = 0.782, Max-TSS = 0.779 and AUC = 0.942 using the repeated split sampling evaluation of the Generic-SDM. While this remains excellent, it is lower than the evaluation scores of the generic SDM. This has two important consequences: first, the species-specific SDM, which does capture the trends in demography along suitability gradients we were expecting, would not be selected based on evaluation metrics, and thus would probably be discarded by a scientist willing to predict its distribution. Second, a demographer willing to interpolate the demography of the species along large geographic distances using SDM-suitability could not use the SDM-evaluation metrics alone to guide their choices.

Supplement S4.4 relationship between SDM-suitability and observed abundance and population growth rates.

Methods

We measured the performance of each populations using six metrics: the observed transient population growth rate, the observed density on the field and the asymptotic population growth rate (predicted by our non-stochastic population model). We extracted the transient population growth rate (the ratio of the observed number of individuals at time t+1 over the number of individuals at time t) for all populations at each observed demographic transitions. The observed population density (number of observed individuals in any given year over the number of plots of the population when observed in the wild) was also extracted for all populations in each observed year. The asymptotic population growth rate was obtained by projecting our structured population model until stable stage (500 iterations) on an identical starting population. We then computed the asymptotic population growth rate as the ratio of the observed number of individuals at time 500 over the number of individuals at time 499, but because of the microsite limited recruitment in our model, it will be equal to one for all populations.

The relationship between observed density and population growth rate and SDM-suitability was assess through a series of linear mixed models with SDM-suitability as a fixed effect and site of origin and year as random factors. The models were fitted using the lme4 package in R (Bates et al. 2015). The relationship between SDM-suitability and the modelled performance metric (the asymptotic population growth rate, the carrying capacity, the average life time reproductive effort and the maximal life time reproductive effort) was computed through linear mixed models. Results are displayed in Figure S4.4.1 and S4.4.2

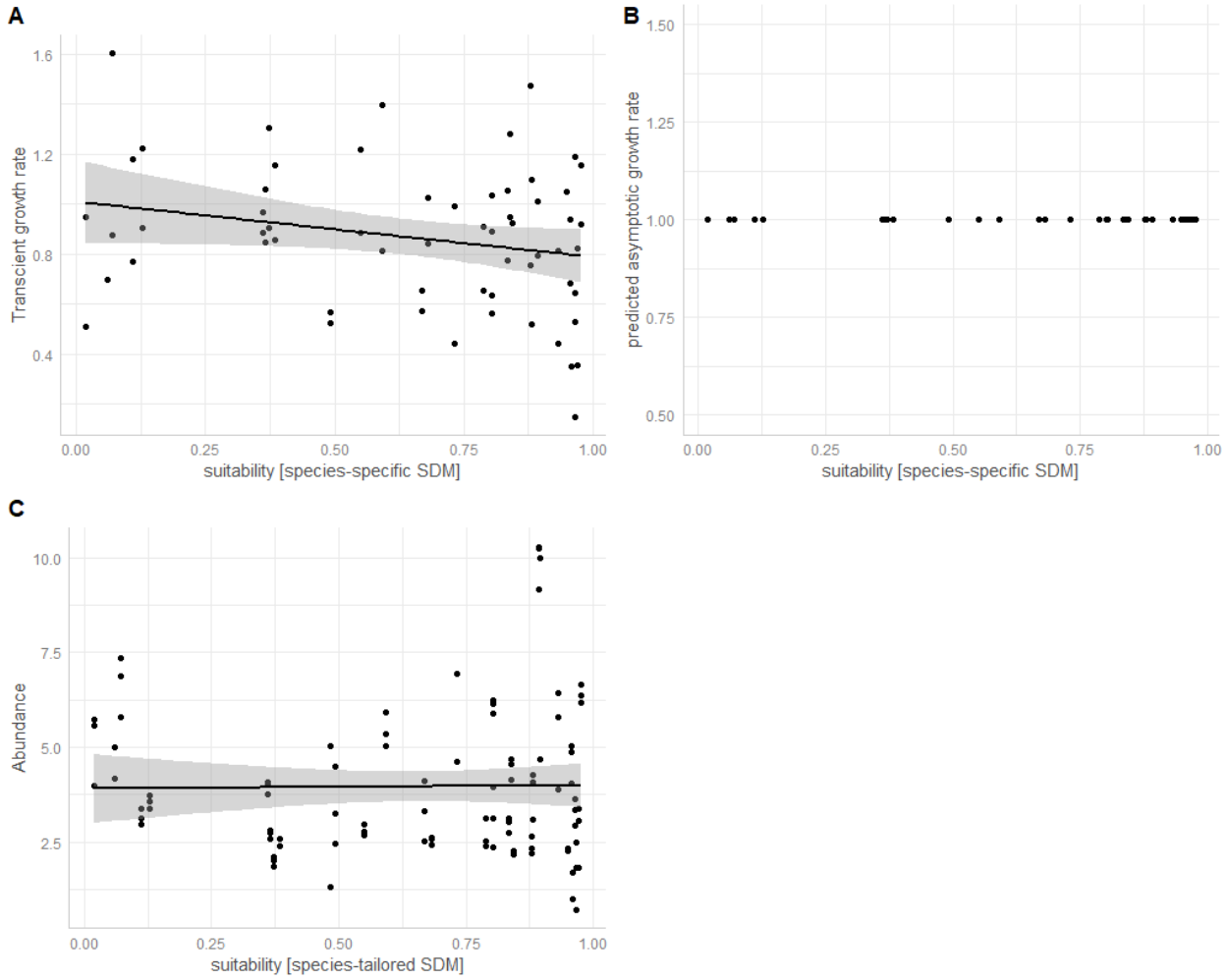

Figure S4.4.1 relationship between population performance and SDM-suitability as predicted by our species-specific SDM. *A) observed population growth rate B) asymptotic population growth rate C) observed population density (number of individuals per 50 cm x 50 cm plot).*

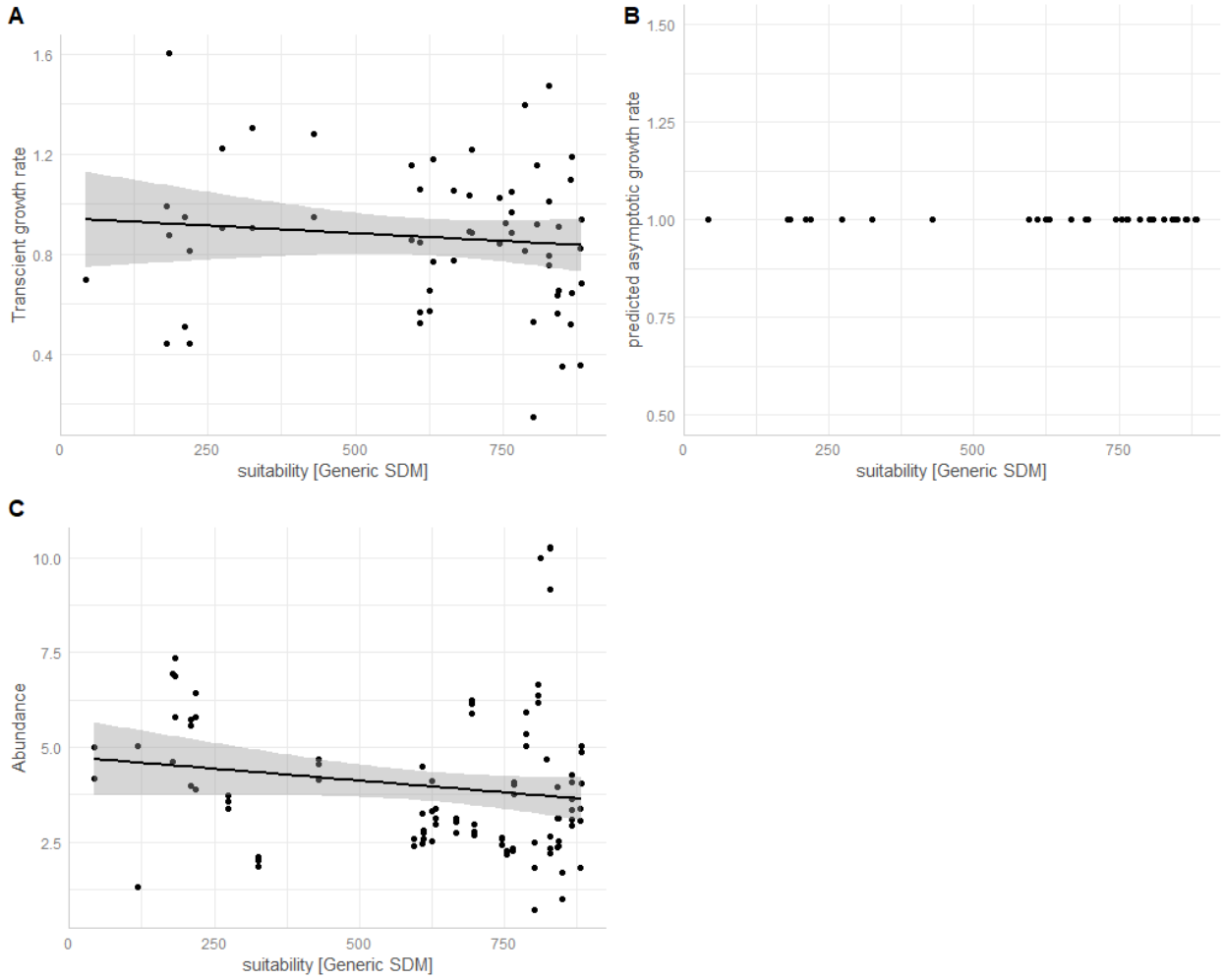

Figure S4.4.2 relationship between population performance and SDM-suitability as predicted by our generic SDM. *A) observed population growth rate B) asymptotic population growth rate C) observed population density (number of individuals per 50 cm x 50 cm plot).*

References for supplements

Bartoń, Kamil. 2018. “MuMIn: Multi-Model Inference Package.”

Bates, Douglas, Martin Mächler, Benjamin M. Bolker, and Steven C. Walker. 2015. “Fitting Linear Mixed-Effects Models Using Lme4.” *Journal of Statistical Software* 67(7):1–48. doi: 10.18637/jss.v067.i01.

Baudraz, Maude E. A., Jean-Nicolas Pradervand, Mélanie Beauverd, Aline Buri, Antoine Guisan, and Pascal Vittoz. 2018. “Learning from Model Errors: Can Land Use, Edaphic and Very High-Resolution Topo-Climatic Factors Improve Macroecological Models of Mountain Grasslands?” *Journal of Biogeography* 45(2):429–37. doi: 10.1111/jbi.13129.

Begon, Michael, Colin R. Townsend, and John L. Harper. 2006. *Ecology : From Individuals to Ecosystems*. 4th ed. Blackwell Publishing.

Beverton, Raymond J. H., and Sidney J. Holt. 1957. *On the Dynamics of Exploited Fish Populations*. Springer Science+Business Media Dordrecht.

Broennimann, O., U. A. Treier, H. Müller-Schärer, W. Thuiller, A. T. Peterson, and A. Guisan. 2007. “Evidence of Climatic Niche Shift during Biological Invasion.” *Ecology Letters* 10(8):701–9. doi: 10.1111/j.1461-0248.2007.01060.x.

Buckley, Yvonne M., Elizabeth E. Crone, Anna Maria Csergő, Johan Ehrlén, Alain Finn, María B. García, Anna-Liisa Laine, Sergi Munné-Bosch, Deborah A. Roach, Jesús Villellas, and Glenda Wardle. 2019. “Plantpopnet Protocol V1.03 2017.” *Figshare*. doi: 10.6084/M9.FIGSHARE.7982477.V9.

Burnham, Kenneth P., and David R. Anderson. 2002. *Model Selection and Multimodel Inference A Practical Information-Theoretic Approach*. Second Ed. New York: Springer.

Chai, T., and R. R. Draxler. 2014. “Root Mean Square Error (RMSE) or Mean Absolute Error (MAE)? -Arguments against Avoiding RMSE in the Literature.” *Geoscientific Model Development* 7(3):1247–50. doi: 10.5194/gmd-7-1247-2014.

Csergő, Anna M., Roberto Salguero-Gómez, Olivier Broennimann, Shaun R. Coutts, Antoine Guisan, Amy L. Angert, Erik Welk, Iain Stott, Brian J. Enquist, Brian McGill, Jens-Christian Svenning, Cyrille Violle, and Yvonne M. Buckley. 2017. “Less Favourable Climates Constrain Demographic Strategies in Plants” edited by J. Gurevitch. *Ecology Letters* 20(8):969–80. doi: 10.1111/ele.12794.

Dubuis, Anne, Sara Giovanettina, Loïc Pellissier, Julien Pottier, Pascal Vittoz, and Antoine Guisan. 2013. “Improving the Prediction of Plant Species Distribution and Community Composition by Adding Edaphic to Topo-Climatic Variables.” *Journal of Vegetation Science* 24(4):593–606. doi: 10.1111/jvs.12002.

Dubuis, Anne, Leila Rossier, Julien Pottier, Loïc Pellissier, Pascal Vittoz, and Antoine Guisan. 2013. “Predicting Current and Future Spatial Community Patterns of Plant Functional Traits.” *Ecography* 36(11):1158–68. doi: 10.1111/j.1600-0587.2013.00237.x.

Elith, Jane, J. R. Leathwick, and T. Hastie. 2008. “A Working Guide to Boosted Regression Trees.” *Journal of Animal Ecology* 77(4):802–13. doi: 10.1111/j.1365-

2656.2008.01390.x.

Garnier, Simon, Noam Ross, Robert Rudis, Antonio Pedro Camargo, Marco Sciaini, and Cédric Scherer. 2021. “Viridis - Colorblind-Friendly Color Maps for R.”

Greenwell, B., B. Boehmke, J. Cunningham, and GBM Developers. 2018. “Gbm: Generalized Boosted Regression Models.”

Guisan, Antoine, Thomas C. Edwards, and Trevor Hastie. 2002. “Generalized Linear and Generalized Additive Models in Studies of Species Distributions: Setting the Scene.” *Ecological Modelling* 157(2–3):89–100. doi: 10.1016/S0304-3800(02)00204-1.

Guisan, Antoine, Wilfried Thuiller, and Niklaus E. Zimmermann. 2017. *Habitat Suitability and Distribution Models with Applications in R*. Cambridge: Cambridge University Press.

Hartig, Florian. 2020. “DHARMa: Residual Diagnostics for Hierarchical (Multi-Level / Mixed) Regression Models.”

Johnson, Paul C. D. 2014. “Extension of Nakagawa & Schielzeth’s R2GLMM to Random Slopes Models.” *Methods in Ecology and Evolution* 5:944–46. doi: 10.1111/2041-210X.12225.

Körner, Christian. 2003. *Alpine Plant Life*. 2nd editio. Berlin.

Kozáková, Radka, Petr Pokorný, Vladimír Peša, Alžběta Danielisová, Katarína Čuláková, and Helena Svitavská Svobodová. 2015. “Prehistoric Human Impact in the Mountains of Bohemia. Do Pollen and Archaeological Data Support the Traditional Scenario of a Prehistoric ‘Wilderness’?” *Review of Palaeobotany and Palynology* 220:29–43. doi: 10.1016/j.revpalbo.2015.04.008.

Kuiper, Pieter Jan Cornelis, and Marten Bos. 1992. *Plantago: A Multidisciplinary Study*. Vol. 89. edited by P. J. C. Kuiper and M. Bos. Springer-Verlag.

Long, Jacob A. 2020. “Jtools: Analysis and Presentation of Social Scientific Data.”

Lüdecke, Daniel. 2018. “Ggeffects: Tidy Data Frames of Marginal Effects from Regression MOdels.” *Journal of Open Source Software* 3(26):772.

Maguire, Bassett. 1973. “Niche Response Structure and the Analytical Potentials of Its Relationship to the Habitat.” *The American Naturalist* 107(954):213–46. doi: 10.1086/282827.

Nakagawa, Shinichi, Paul C. D. Johnson, and Holger Schielzeth. 2017. “The Coefficient of Determination R2 and Intra-Class Correlation Coefficient from Generalized Linear Mixed-Effects Models Revisited and Expanded.” *Journal of the Royal Society Interface* 14(134). doi: 10.1098/rsif.2017.0213.

Nakagawa, Shinichi, and Holger Schielzeth. 2013. “A General and Simple Method for Obtaining R 2 from Generalized Linear Mixed-Effects Models.” *Methods in Ecology and Evolution* 4(2):133–42. doi: 10.1111/j.2041-210x.2012.00261.x.

Petitpierre, B., C. Kueffer, O. Broennimann, C. Randin, C. Daehler, and A. Guisan. 2012. “Climatic Niche Shifts Are Rare Among Terrestrial Plant Invaders.” *Science*

335(6074):1344–48. doi: DOI 10.1126/science.1215933.

Phillips, Steven J., Robert P. Anderson, and Robert E. Schapire. 2006. “Maximum Entropy Modeling of Species Geographic Distributions.” *Ecological Modelling* 190(3–4):231–59. doi: 10.1016/J.ECOLMODEL.2005.03.026.

Prasad, Anantha M., Louis R. Iverson, and Andy Liaw. 2006. “Newer Classification and Regression Tree Techniques: Bagging and Random Forests for Ecological Prediction.” *Ecosystems 2006 9:2* 9(2):181–99. doi: 10.1007/S10021-005-0054-1.

Randin, Christophe F., Hélène Jaccard, Pascal Vittoz, Nigel G. Yoccoz, and Antoine Guisan. 2009. “Land Use Improves Spatial Predictions of Mountain Plant Abundance but Not Presence-Absence.” *Journal of Vegetation Science* 20(6):996–1008. doi: 10.1111/j.1654-1103.2009.01098.x.

Roberts, David R., Volker Bahn, Simone Ciuti, Mark S. Boyce, Jane Elith, Gurutzeta Guillera-Arroita, Severin Hauenstein, José J. Lahoz-Monfort, Boris Schröder, Wilfried Thuiller, David I. Warton, Brendan A. Wintle, Florian Hartig, and Carsten F. Dormann. 2017. “Cross-Validation Strategies for Data with Temporal, Spatial, Hierarchical, or Phylogenetic Structure.” *Ecography* 40(8):913–29. doi: 10.1111/ECOG.02881.

Thuiller, Wilfried, Damien Georges, Robin Engler, and Franck Breiner. 2016. “Biomod2: Ensemble Platform for Species Distribution Modeling. R Package Version 2:R560.”

Thuiller, Wilfried, David M. Richardson, Petr Pyšek, Guy F. Midgley, Grego O. Hughes, and Mathieu Rouget. 2005. “Niche-Based Modelling as a Tool for Predicting the Risk of Alien Plant Invasions at a Global Scale.” *Global Change Biology* 11(12):2234–50. doi: 10.1111/J.1365-2486.2005.001018.X.

Valavi, Roozbeh, Jane Elith, José J. Lahoz-Monfort, and Gurutzeta Guillera-Arroita. 2019. “BlockCV: An r Package for Generating Spatially or Environmentally Separated Folds for k-Fold Cross-Validation of Species Distribution Models.” *Methods in Ecology and Evolution* 10(2):225–32. doi: 10.1111/2041-210X.13107.

Villellas, Jesús, Johan Ehrlén, Elizabeth E. Crone, Anna Mária Csergő, Maria B. Garcia, Anna Liisa Laine, Deborah A. Roach, Roberto Salguero-Gómez, Glenda M. Wardle, Dylan Z. Childs, Bret D. Elderd, Alain Finn, Sergi Munné-Bosch, Benedicte Bachelot, Judit Bódis, Anna Bucharova, Christina M. Caruso, Jane A. Catford, Matthew Coghill, Aldo Compagnoni, Richard P. Duncan, John M. Dwyer, Aryana Ferguson, Lauchlan H. Fraser, Emily Griffoul, Ronny Groenteman, Liv Norunn Hamre, Aveliina Helm, Ruth Kelly, Lauri Laanisto, Michele Lonati, Zuzana Münzbergová, Paloma Nuche, Siri Lie Olsen, Adrian Oprea, Meelis Pärtel, William K. Petry, Satu Ramula, Pil U. Rasmussen, Simone Ravetto Enri, Anna Roeder, Christiane Roscher, Cheryl Schultz, Olav Skarpaas, Annabel L. Smith, Ayco J. M. Tack, Joachim P. Töpper, Peter A. Vesk, Gregory E. Vose, Elizabeth Wandrag, Astrid Wingler, and Yvonne M. Buckley. 2021. “Phenotypic Plasticity Masks Range-Wide Genetic Differentiation for Vegetative but Not Reproductive Traits in a Short-Lived Plant.” *Ecology Letters* 24(11):2378–93.

Willmott, Cort J., and Kenji Matsuura. 2005. “Advantages of the Mean Absolute Error (MAE) over the Root Mean Square Error (RMSE) in Assessing Average Model Performance.” *Climate Research* 30(1):79–82. doi: 10.3354/cr030079.

Wu, Lin, and Janis Antonovics. 1976. “Experimental Ecological Genetics in Plantago II . Lead Tolerance in Plantago Lanceolata and Cynodon Dactylon from a Roadside Author (s): Lin Wu and Janis Antonovics Published by : Ecological Society of America.” *Ecology* 57(1):205–8.

Zimmermann, Niklaus E., T. C. Edwards, G. G. Moisen, T. S. Frescino, and J. A. Blackward. 2007. “Remote Sensing-Based Predictors Improve Distribution Models of Rare, Early Successional and Broadleaf Tree Species in Utah.” *The Journal of Applied Ecology* 44(5):1057–67. doi: 10.1111/J.1365-2664.2007.01348.X.

Zimmermann, Niklaus E., and Felix Kienast. 1999. “Predictive Mapping of Alpine Grasslands in Switzerland: Species versus Community Approach.” *Journal of Vegetation Science* 10(4):469–82. doi: 10.2307/3237182.